

# Influence of Charge on Decoupled Anisotropic Spheres in $f(G, T)$ Gravity

M. Sharif<sup>1</sup> \*and K. Hassan<sup>2</sup> †

<sup>1</sup> Department of Mathematics and Statistics, The University of Lahore, 1-KM Defence Road Lahore, Pakistan.

<sup>2</sup> Department of Mathematics, University of the Punjab, Quaid-e-Azam Campus, Lahore-54590, Pakistan.

## Abstract

In this paper, we develop two anisotropic solutions for static self-gravitating spherical structure in the presence of electromagnetic field through gravitational decoupling approach in  $f(G, T)$  theory, where  $G$  and  $T$  denote the Gauss-Bonnet term and trace of the energy-momentum tensor, respectively. The extra source with isotropic seed sector is responsible for generating anisotropy in the spacetime. The system of field equations is decoupled into two arrays by using minimal geometric deformation in the radial component. The first set portrays the isotropic regime whereas the second set represents the anisotropic system. The metric coefficients of the Krori-Barua spacetime are employed to extract solution of the first set while two constraints on the radial and temporal components of the extra source yield the corresponding two solutions. Finally, we investigate the influence of charge and decoupling parameter on the physical viability and stability of the obtained solutions. We conclude that the resulting solutions in this modified theory indicate more feasible and stable structures.

**Keywords:** Self-gravitating systems; Gravitational decoupling;  $f(G, T)$  gravity.

**PACS:** 04.20.Jb; 04.40.Dg; 04.50.Kd

---

\*msharif.math@pu.edu.pk

†komalhassan3@gmail.com

# 1 Introduction

The immense and perplexing universe is composed of large-scale structures such as clouds, stars, galaxies and clusters of galaxies. General theory of relativity (GR) has played a crucial role to examine the properties and mechanism of the cosmos. Dark energy and dark matter with mysterious properties are assumed to be well described by this theory to resolve the flat rotation curves of galaxies [1] along with late-time acceleration of the universe [2]. The Lambda cold dark matter model was developed to elucidate the occurrence of dark energy by incorporating the cosmological constant. In order to conform the values of cosmological constant with the observational data and to elaborate the evolution of the universe through various cosmic eras, its value should be readapted. To address these problems, many researchers have suggested to modify GR by changing the Einstein-Hilbert action.

The first and second-order terms in Lovelock gravity [3], a higher dimensional generalization of GR, represent GR and Gauss-Bonnet (GB) invariant, respectively. Mathematically, in four dimensions, the GB term is denoted as  $G = R^2 - 4R^{\psi\chi}R_{\psi\chi} + R^{\psi\chi\nu\mu}R_{\psi\chi\nu\mu}$  which is a combination of of the Ricci tensor ( $R_{\psi\chi}$ ), Riemann tensor ( $R_{\psi\chi\nu\mu}$ ) and Ricci scalar ( $R$ ). Nojiri and Odintsov [4] formulated  $f(G)$  gravity or modified GB theory by including the generic function  $f(G)$  in the Einstein-Hilbert action. Modified theories with curvature-matter coupling are considered as viable techniques that might elucidate the remarkable phenomena of rapid cosmic expansion. Sharif and Ikram [5] proposed  $f(G, T)$  gravity by including a generalized  $f(G, T)$  function in the Einstein-Hilbert action and discussed energy conditions in the context of FRW universe. The non-zero divergence of the energy-momentum tensor (EMT) creates an extra force that leads test particles to trace the non-geodesic paths. The same authors [6] studied wormholes by considering a variety of matter configurations. Yousaf et al. [7] examined physical properties of the stellar entities by decomposing the Riemann tensor in this framework for charged/uncharged spherical system. Sharif and Hassan [8] studied the complexity factor for a non-static spherical and static/non-static cylindrical structures.

The inclusion of the electromagnetic field in celestial formations has an interesting impact for studying and analyzing their evolution. There has been a large body of literature to study the influence of charge on stellar bodies in GR as well as modified theories. Xingxiang [9] discussed static sphere constituting charged perfect fluid. Das et al. [10] studied charged

static spherical solutions by matching the interior geometry with the exterior Riessner-Nordström metric. Sharif and Bhatti [11] numerically solved the field equations for a shearfree charged object and checked the viability through the energy conditions. Murad [12] explored anisotropic charged celestial objects by assuming a specific form of a metric potential. Different aspects describing the internal structure of self-gravitating bodies have been examined in the presence of an electric field [13].

The presence of interacting substance in dense compact structures reveals that they display different properties in various directions which depicts the anisotropic nature of the compact objects [14]. Phase transition [15] and superfluid [16] are considered the reasons to produce anisotropy in the system. Herrera and Santos [17] investigated the origin of anisotropy and inspected its influence in the evolution of self-gravitating bodies. Harko and Mak [18] determined the analytic solution of the field equations by employing a particular anisotropic factor and analyzed the static spherical anisotropic configurations. Paul and Deb [19] investigated physical attributes of anisotropic star models in hydrostatic equilibrium.

The analytic solutions to the field equations help us to understand the intricate nature of the self-gravitating bodies. However, it is often difficult to obtain solutions of the field equations due to their non-linearity. The gravitational decoupling via minimal geometric deformation (MGD) is the recently developed approach to find viable solutions. In this approach, the radial function of the line element is distorted by means of a linear transformation which segregates the system of field equations into two sets. The first set describes the seed sector, and the second corresponds to the extra source. Both these sets are addressed independently and the solution of the whole system is determined by applying the superposition principle. Ovalle [20] was the pioneer to develop this scheme in the context of braneworld to calculate the exact solutions of celestial objects. Later, Ovalle et al. [21] investigated the feasibility of a celestial object in GR by extending the isotropic domain to anisotropic configuration. Gabbanelli et al. [22] used the Durgapal-Fuloria solution to determine its anisotropic version using the same technique.

Sharif and Sadiq [23] studied the impact of charge and formulated two anisotropic solutions using Krori-Barua spacetime via MGD method. Estrada and Tello-Ortiz [24] used Heintzmann solution to develop two consistent anisotropic solutions. Singh et al. [25] developed physically acceptable solutions through this approach for class-I spacetime and determined the mass and radius of the stars by plotting  $M$ - $R$  curve. Hensh and Stuchlík [26]

worked on isotropic Tolman VII solution to calculate its anisotropic version by using the decoupling method. Zubair and Azmat [27] constructed the anisotropic solution by deforming the radial function of isotropic Tolman V solution. Maurya and his collaborators [28] worked on the MGD technique to formulate the anisotropic solutions from known isotropic domain in different modified theories. Sharif and Saba [29] constructed charged/uncharged gravitational decoupled anisotropic solutions from a known isotropic solution and examined the viability and stability of the obtained solutions in the framework of  $f(G)$  gravity. Many researchers obtained anisotropic versions of the isotropic source and checked the feasibility conditions of compact stars in the formalism of different modified theories [30]. We have recently studied decoupled anisotropic spheres in  $f(G, T)$  gravity [31].

This paper deals with the deformation of the radial component of Krori-Barua metric through MGD scheme to extract charged anisotropic solutions in  $f(G, T)$  gravity. The format of the paper is as follows. Section **2** addresses the key features of this modified theory. In section **3**, the MGD procedure splits the field equations into two arrays in which one describes the isotropic source while the other represents the anisotropic configuration. We obtain anisotropic solutions by using two constraints on radial as well as temporal components of the extra source in section **4**. The physical viability and stability of the constructed solutions are examined in section **5**. In the last section, we summarize our results.

## 2 $f(G, T)$ Formalism

The  $f(G, T)$  field equations are acquired with the help of modified action as

$$\mathbb{A}_{f(G,T)} = \int \sqrt{-g} d^4x \left[ \frac{R + f(G, T)}{16\pi} + \mathcal{L}_m + \mathcal{L}_E + \xi \mathcal{L}_\omega \right], \quad (1)$$

where determinant of the metric tensor ( $g_{\psi\chi}$ ) and matter Lagrangian density are represented by  $g$  and  $\mathcal{L}_m$ , respectively. The Lagrangian density of the electromagnetic field and additional source are specified by  $\mathcal{L}_E$  and  $\mathcal{L}_\omega$ , respectively, whereas  $\xi$  denotes the decoupling parameter. The corresponding EMT of the sources are given by the relation

$$T_{\psi\chi} = g_{\psi\chi} \mathcal{L}_m - \frac{2\partial \mathcal{L}_m}{\partial g^{\psi\chi}}, \quad \omega_{\psi\chi} = g_{\psi\chi} \mathcal{L}_\omega - \frac{2\partial \mathcal{L}_\omega}{\partial g^{\psi\chi}}. \quad (2)$$

By varying the action (1) with respect to  $g_{\psi\chi}$ , we obtain the modified field equations as

$$G_{\psi\chi} = 8\pi T_{\psi\chi}^{(tot)} = 8\pi(T_{\psi\chi}^{(D)} + T_{\psi\chi}^{(M)} + E_{\psi\chi} + \xi\omega_{\psi\chi}), \quad (3)$$

where  $G_{\psi\chi} = R_{\psi\chi} - \frac{1}{2}Rg_{\psi\chi}$  indicates the Einstein tensor and  $T_{\psi\chi}^{(D)}$  demonstrates the correction terms caused by  $f(G, T)$  theory as

$$\begin{aligned} T_{\psi\chi}^{(D)} &= \frac{1}{8\pi} \left[ \{(\mu + P)v_\psi v_\chi\} f_T(G, T) + \frac{1}{2}g_{\psi\chi} f(G, T) + (4R^{\alpha\nu} R_{\psi\alpha\chi\nu} \right. \\ &\quad - 2RR_{\psi\chi} - 2R_{\psi}^{\alpha\nu\gamma} R_{\chi\alpha\nu\gamma}) f_G(G, T) + 4R_{\alpha\chi} R_{\psi}^{\alpha} + (4g_{\psi\chi} R^{\alpha\nu} \nabla_\alpha \nabla_\nu \\ &\quad - 4R_{\psi}^{\alpha} \nabla_\chi \nabla_\alpha - 4R_{\psi\alpha\chi\nu} \nabla^\alpha \nabla^\nu - 2g_{\psi\chi} R \nabla^2 + 2R \nabla_\psi \nabla_\chi - 4R_{\chi}^{\alpha} \nabla_\psi \nabla_\alpha \\ &\quad \left. + 4R_{\psi\chi} \nabla^2) f_G(G, T) \right], \quad (4) \end{aligned}$$

$\nabla^2 = \nabla^b \nabla_b$  signifies the d' Alembert operator. Further,  $f_G(G, T)$  and  $f_T(G, T)$  denote the partial derivatives of an arbitrary function  $f(G, T)$  with respect to  $G$  and  $T$ , respectively. An additional source  $\omega_{\psi\chi}$  is found to be responsible for inducing anisotropy in the current scenario which is associated with the seed sector via dimensionless parameter  $\xi$ .

The EMT plays a significant role in determining the internal configuration of the celestial bodies. In the current setup, the perfect fluid source is presented by the EMT

$$T_{\psi\chi}^{(M)} = (\mu + P)v_\psi v_\chi + Pg_{\psi\chi}, \quad (5)$$

where  $\mu$ ,  $P$  and  $v^\psi$  indicate the density, pressure and four-velocity, respectively, satisfying  $v^\psi v_\psi = -1$ . The tensor  $E_{\psi\chi}$  describes EMT for the electromagnetic field as

$$E_{\psi\chi} = \frac{1}{4\pi} \left( F_{\psi}^l F_{\chi l} - \frac{1}{4} F_{lm} F^{lm} g_{\psi\chi} \right), \quad (6)$$

where  $F_{\psi\chi} = \gamma_{\chi,\psi} - \gamma_{\psi,\chi}$  and  $\gamma_\psi$  indicate the Maxwell field tensor and four potential, respectively. Here we take  $\gamma_\psi = \gamma(r)\delta_\psi^0$ . The tensorial form of the Maxwell field equations are expressed as

$$F^{\psi\chi}_{;\chi} = 4\pi J^\psi, \quad F_{[\psi\chi;l]} = 0,$$

where  $J^\psi = \sigma v^\psi$  is the four current density while  $\sigma$  denotes the charge density. The viability and stability of the resulted anisotropic solutions will be checked by assuming an explicit model of  $f(G, T)$  gravity [32] as

$$f(G, T) = \mathbf{f}_1(G) + \mathbf{f}_2(T), \quad (7)$$

where  $\mathbf{f}_1(G)$  and  $\mathbf{f}_2(T)$  are independent functions of  $G$  and  $T$ , respectively. There can be many choices regarding curvature and matter coupling, however, in order to consider its role more effectively, we assume a quadratic  $f(G, T)$  model. For this purpose, we choose  $\mathbf{f}_1(G) = G^2$  and  $\mathbf{f}_2(T) = \beta T$ , where  $\beta$  refers to a free parameter. The values of  $G$  and its higher derivatives are provided in Eqs.(A1)-(A3) of Appendix A.

The interior region of the spherical compact object is given by

$$ds^2 = -e^\phi dt^2 + e^\lambda dr^2 + r^2(d\theta^2 + \sin^2\theta d\Phi^2), \quad (8)$$

where  $\phi$  and  $\lambda$  are functions of  $r$  only. The Maxwell field equations give

$$\gamma'' + \left( \frac{2}{r} - \frac{\phi' + \lambda'}{2} \right) \gamma' = 4\pi\sigma e^{\frac{\phi}{2} + \lambda}, \quad (9)$$

prime means derivative with respect to  $r$  and its integration leads to

$$\gamma' = \frac{se^{\frac{\phi+\lambda}{2}}}{r^2}, \quad (10)$$

$s$  denotes the presence of charge in the interior of self-gravitating body. The components of four-velocity in the comoving frame take the form

$$v^\psi = \left( e^{-\frac{\phi}{2}}, 0, 0, 0 \right). \quad (11)$$

The corresponding field equations are

$$\frac{1}{r^2} + e^{-\lambda} \left( \frac{\lambda'}{r} - \frac{1}{r^2} \right) = 8\pi \left( \bar{\mu} + \frac{s^2}{8\pi r^4} + T_0^{0(D)} - \xi\omega_0^0 \right), \quad (12)$$

$$-\frac{1}{r^2} + e^{-\lambda} \left( \frac{1}{r^2} + \frac{\phi'}{r} \right) = 8\pi \left( \bar{P} - \frac{s^2}{8\pi r^4} + T_1^{1(D)} + \xi\omega_1^1 \right), \quad (13)$$

$$e^{-\lambda} \left( \frac{\phi''}{2} + \frac{\phi'^2}{4} - \frac{\lambda'\phi'}{4} + \frac{\phi'}{2r} - \frac{\lambda'}{2r} \right) = 8\pi \left( \bar{P} + \frac{s^2}{8\pi r^4} + T_2^{2(D)} + \xi\omega_2^2 \right), \quad (14)$$

where

$$\bar{\mu} = \mu + \frac{\beta}{16\pi}(3\mu - P), \quad \bar{P} = P + \frac{\beta}{16\pi}(-\mu + 3P), \quad (15)$$

and the extra curvature terms  $T_0^{0(D)}$ ,  $T_1^{1(D)}$  and  $T_2^{2(D)}$  are mentioned in Eqs.(A4)-(A6) of Appendix **A**.

Unlike GR,  $f(G, T)$  theory yields the non-conserved form of EMT which, in return, produces the additional force. The non-conservation of the matter source is represented by the equation

$$\begin{aligned} \nabla^\psi T_{\psi\chi} &= \frac{f_T(G, T)}{k^2 - f_T(G, T)} \left[ -\frac{1}{2}g_{\psi\chi} \nabla^\psi T + (\Theta_{\psi\chi} + T_{\psi\chi}) \nabla^\psi (\ln f_T(G, T)) \right. \\ &\quad \left. + \nabla^\psi \Theta_{\psi\chi} \right], \end{aligned} \quad (16)$$

yielding

$$\frac{dP}{dr} + \frac{\lambda'}{2}(\mu + P) + \xi \frac{d\omega_1^1}{dr} - \frac{ss'}{4\pi r^4} + \frac{\xi\lambda'}{2}(\omega_1^1 - \omega_0^0) + \frac{2\xi}{r}(\omega_1^1 - \omega_2^2) = \Omega, \quad (17)$$

where  $\Omega$  includes the contribution of extra curvature terms given in Eq.(A7) of Appendix **A**. The system of non-linear differential equations (12)-(14) together with (17) have eight unknowns, showing that our system is under-determined (more unknowns than equations), therefore, we need more constraints to solve the system. For this purpose, we employ the systematic approach of MGD to close our system. We reformulate the physical variables as

$$\tilde{\mu} = \mu - \xi\omega_0^0, \quad \tilde{P}_r = P + \xi\omega_1^1, \quad \tilde{P}_t = P + \xi\omega_2^2, \quad (18)$$

where  $\omega_\chi^\psi$  is the anisotropy producing factor for the astrophysical objects. The effective anisotropy is defined as

$$\tilde{\Delta} = \tilde{P}_t - \tilde{P}_r = \xi(\omega_2^2 - \omega_1^1), \quad (19)$$

which will be zero for  $\xi = 0$ .

### 3 Gravitational Decoupling Via MGD

Here, we apply the gravitational decoupling through MGD scheme to solve the system (12)-(14) and evaluate the unknowns (physical variables, metric potentials, charge and anisotropic source). This approach splits the

field equations in such a way that the extra source  $\omega_\chi^\psi$  is found to generate anisotropy in the internal geometry. We start with the solution of perfect matter configuration by the following line element

$$ds^2 = -e^{\vartheta(r)} dt^2 + \frac{dr^2}{\tau(r)} + r^2(d\theta^2 + \sin^2\theta d\Phi^2), \quad (20)$$

where  $\tau(r) = 1 - \frac{2m}{r} + \frac{s^2}{r^2}$  and  $m(r)$  corresponds to the Misner-Sharp mass of the compact object. We distort the metric potentials to comprehend the influence of anisotropy on the perfect matter by utilizing the linear transformations as

$$\vartheta \rightarrow \phi = \vartheta + \xi k, \quad \tau \rightarrow e^{-\lambda(r)} = \tau + \xi h^*, \quad (21)$$

where  $k$  and  $h^*$  are the deformations assigned to the temporal and radial metric functions, respectively. In MGD, only radial potential is translated, i.e.,  $k = 0$  which means that the temporal part remains unperturbed. The field equations (12)-(14) are segregated into two sets by using the deformed metric. By substituting  $\xi = 0$ , the modified field equations for the perfect fluid yield the first set as

$$8\pi\left(\mu + \frac{\beta}{16\pi}(3\mu - P) + \frac{s^2}{8\pi r^4} + T_0^{0(D)}\right) = \frac{1}{r^2} - \left(\frac{\tau'}{r} + \frac{\tau}{r^2}\right), \quad (22)$$

$$8\pi\left(P + \frac{\beta}{16\pi}(-\mu + 3P) - \frac{s^2}{8\pi r^4} + T_1^{1(D)}\right) = -\frac{1}{r^2} + \frac{\tau}{r}\left(\frac{1}{r} + \phi'\right), \quad (23)$$

$$8\pi\left(P + \frac{\beta}{16\pi}(-\mu + 3P) + \frac{s^2}{8\pi r^4} + T_2^{2(D)}\right) = \tau\left(\frac{\phi''}{2} + \frac{\phi'^2}{4} + \frac{\phi'}{2r}\right) + \tau'\left(\frac{\phi'}{4} + \frac{1}{2r}\right). \quad (24)$$

Solving the above equations simultaneously, the expressions for  $\mu$ ,  $P$  and  $s^2$  become

$$\begin{aligned} \mu = & \frac{-1}{16(\beta^2 + 12\pi\beta + 32\pi^2)r^2} \left[ \beta r^2 \tau' \phi' - 4\beta + 2\beta r^2 \tau \phi'' + \beta r^2 \tau \phi'^2 \right. \\ & + 8\pi r^2 \tau' \phi' + 16\pi r^2 \tau \phi'' + 8\pi r^2 \tau \phi'^2 + (12\beta r^2 + 64\pi r^2) T_0^{0(D)} + (8\beta r^2 \\ & + 32\pi r^2) T_1^{1(D)} - 32\pi(-4\beta r^2 - 32\pi r^2) T_2^{2(D)} + 14\beta r \tau' - 6\beta r \tau \phi' + 4\beta \tau \\ & \left. + 80\pi r \tau' - 16\pi r \tau \phi' + 32\pi \tau \right], \quad (25) \end{aligned}$$

$$P = \frac{-1}{16(\beta + 4\pi)(\beta + 8\pi)r^2} \left[ 4\beta - \beta r^2 \tau' \phi' - 2\beta r^2 \tau \phi'' - \beta r^2 \tau \phi'^2 - 16\pi r^2 \tau \phi'' \right. \\ \left. - 8\pi r^2 \tau' \phi' - 8\pi r^2 \tau \phi'^2 + 4\beta r^2 T_0^{0(D)} + (8\beta r^2 + 32\pi r^2) T_1^{1(D)} + 2\beta r \tau' - 4\beta \tau \right. \\ \left. + (4\beta r^2 + 32\pi r^2) T_2^{2(D)} - 10\beta r \tau \phi' - 16\pi r \tau' - 48\pi r \tau \phi' - 32\pi \tau + 32\pi \right], \quad (26)$$

$$s^2 = \frac{1}{8} \left( r^4 \tau' \phi' + 2r^4 \tau \phi'' + r^4 \tau \phi'^2 + 4r^4 T_1^{1(D)} - 4r^4 T_2^{2(D)} + 2r^3 \tau' - 2r^3 \tau \phi' \right. \\ \left. - 4r^2 \tau + 4r^2 \right). \quad (27)$$

The anisotropy generated by the new source is studied by the second set

$$8\pi\omega_0^0 = \frac{h^*}{r} + \frac{h^*}{r^2}, \quad (28)$$

$$8\pi\omega_1^1 = \frac{h^*}{r} \left( \frac{1}{r} + \phi' \right), \quad (29)$$

$$8\pi\omega_2^2 = h^* \left( \frac{\phi''}{2} + \frac{\phi'^2}{4} + \frac{\phi'}{2r} \right) + h^{*'} \left( \frac{\phi'}{4} + \frac{1}{2r} \right). \quad (30)$$

One can observe that the above system of field equations seems similar for the charged spherical anisotropic matter source through the metric

$$ds^2 = -e^{\vartheta(r)} dt^2 + \frac{dr^2}{h^*} + r^2 (d\theta^2 + \sin^2 \theta d\Phi^2). \quad (31)$$

It can also be noted that the term  $\frac{1}{r^2}$  is the only varying quantity between Eqs.(22)-(23) and (28)-(29). In order to make this system equivalent to the standard field equations for charged anisotropic stellar object, we specify the physical variables as  $\bar{\mu} + \frac{s^2}{8\pi r^4} = \omega_0^{*0} = \omega_0^0 + \frac{1}{r^2}$ ,  $\bar{P}_r - \frac{s^2}{8\pi r^4} = \omega_1^{*1} = \omega_1^1 + \frac{1}{r^2}$ , and  $\bar{P}_t + \frac{s^2}{8\pi r^4} = \omega_2^{*2} = \omega_2^2 = \omega_3^{*3} = \omega_3^3$ .

Junction conditions play a crucial role in understanding the fundamental characteristics of the astrophysical objects at the boundary ( $\Sigma$ ). The first and second fundamental forms of junction conditions assure the smooth matching of exterior and interior geometries at the junction. The choice of an outer region is examined on the basis that its properties (static, irrotational, charged) at the hypersurface match with the interior regime. The matter source is restricted only within the stellar object, and a boundary is marked with the outer Reissner-Nordström (presence of charge in the exterior region) metric to separate both the structures. In the scenario of  $f(G, T)$

theory, the inclusion of higher curvature terms in  $G$  will be significantly restrained and there is no contribution of  $T$  in charged spacetime. Hence, the external geometry as in GR can be chosen for modified theories. Furthermore, the Reissner-Nordström metric has been used in the literature for  $f(G)$  and  $f(G, T)$  gravity theories with the same spacetime [33]. We choose the interior region as

$$ds^2 = -e^{\phi(r)} dt^2 + \frac{1}{\left(1 - \frac{2\tilde{m}}{r} + \frac{s^2}{r^2}\right)} dr^2 + r^2(d\theta^2 + \sin^2\theta d\Phi^2), \quad (32)$$

where  $\tilde{m} = m(r) - \frac{\xi r}{2} h^*(r)$  indicates the inner geometric mass. The matching of the first fundamental form ( $[ds^2 = 0]_\Sigma$ ) at the boundary ( $r = R$ ) of the stellar object yields

$$\phi_-(R) = \phi_+(R), \quad e^{-\lambda_+(R)} = e^{-\lambda_-(R)} = 1 - \frac{2M_o}{R} + \frac{S_o^2}{R^2} + \xi h^*(R), \quad (33)$$

where  $\tau = e^{-\lambda} - \xi h^*$  has been utilized. Here, plus and minus signs in the metric potentials indicate the exterior and interior regions, respectively. Moreover,  $M_o = m(R)$ ,  $S_o^2 = s^2(R)$  and  $h^*(R)$  represent the total mass, charge and deformation function at the boundary of the star. The matching of the second fundamental form ( $[(T_{\psi\chi}^{(tot)} W^\chi)_\Sigma = 0, (W^\chi = (0, e^{-\frac{\lambda}{2}}, 0, 0))]$ ) at the hypersurface yields

$$\bar{P}(R) - \frac{S_o^2}{8\pi R^4} + \xi(\omega_1^1(R))_- + (T_1^{1(D)}(R))_- = \xi(\omega_1^1(R))_+ + (T_1^{1(D)}(R))_+. \quad (34)$$

Using Eq.(33) in the above equation, we have

$$\bar{P}(R) - \frac{S_o^2}{8\pi R^4} + \xi(\omega_1^1(R))_- = \xi(\omega_1^1(R))_+, \quad (35)$$

which can be also be expressed as

$$\bar{P}(R) - \frac{S_o^2}{8\pi R^4} + \frac{\xi h^*(R)}{8\pi} \left(\frac{\phi'}{R} + \frac{1}{R^2}\right) = \frac{\xi a^*(R)}{8\pi R} \left(\frac{1}{R} + \frac{2M - \frac{2S^2}{R}}{R(R - 2M) + S^2}\right). \quad (36)$$

Here  $M$  and  $S$  indicate the mass and charge of the exterior geometry, respectively, while  $a^*$  corresponds to the outer radial geometric deformation. The

external geometric structure representing the impact of anisotropic matter configuration is expressed by the Reissner-Nordström spacetime

$$ds^2 = -\left(1 - \frac{2\mathbb{M}}{r} + \frac{\mathcal{S}^2}{r^2}\right) dt^2 + \frac{1}{\left(1 - \frac{2\mathbb{M}}{r} + \frac{\mathcal{S}^2}{r^2} + \xi a^*\right)} dr^2 + r^2(d\theta^2 + \sin^2\theta d\Phi^2). \quad (37)$$

The necessary and sufficient requirements are provided by Eqs.(33) and (36) to remove any discontinuity or irregularity at the boundary. The assumption ( $a^* = 0$ ) converts Eq.(36) to the standard Reissner-Nordström case as

$$\tilde{P}(\mathbb{R}) - \frac{\mathcal{S}_o^2}{8\pi\mathbb{R}^4} = \bar{P}(\mathbb{R}) - \frac{\mathcal{S}_o^2}{8\pi\mathbb{R}^4} + \frac{\xi h^*(\mathbb{R})}{8\pi} \left(\frac{\phi'}{\mathbb{R}} + \frac{1}{\mathbb{R}^2}\right) = 0. \quad (38)$$

## 4 Anisotropic Solutions

In this section, we evaluate the anisotropic charged spherical solutions by using the isotropic (seed) solution called Krori-Barua metric [34] which has a singularity-free nature. This is given by

$$e^{\phi(r)} = e^{\mathcal{B}r^2 + \mathcal{C}}, \quad e^{\lambda(r)} = \tau^{-1} = e^{\mathcal{A}r^2}. \quad (39)$$

Using this solution in the field equations (22)-(24), we obtain

$$\begin{aligned} \mu = \frac{1}{4(\beta^2 + 12\pi\beta + 32\pi^2)r^2} & \left[ e^{-\mathcal{A}r^2} \left( -8\pi \left( -\mathcal{A}r^2(\mathcal{B}r^2 + 5) + e^{\mathcal{A}r^2} (r^2(2 \right. \right. \right. \\ & \times T_0^{0(D)} + T_1^{1(D)} - T_2^{2(D)}) - 1) + \mathcal{B}^2 r^4 + 1) - \beta \left( -\mathcal{A}r^2(\mathcal{B}r^2 + 7) + e^{\mathcal{A}r^2} \right. \\ & \left. \left. \left. \times (r^2(3T_0^{0(D)} + 2T_1^{1(D)} - T_2^{2(D)}) - 1) + (\mathcal{B}r^2 - 1)^2 \right) \right) \right], \quad (40) \end{aligned}$$

$$\begin{aligned} P = \frac{1}{4(\beta + 4\pi)(\beta + 8\pi)r^2} & \left[ e^{-\mathcal{A}r^2} \left( -\beta(\mathcal{A}\mathcal{B}r^4 + e^{\mathcal{A}r^2} (r^2(T_0^{0(D)} + 2T_1^{1(D)} + T_2^{2(D)} \right. \right. \right. \\ & + 1) - \mathcal{A}r^2 - \mathcal{B}^2 r^4 - 6\mathcal{B}r^2 - 1) - 8\pi(\mathcal{A}\mathcal{B}r^4 + e^{\mathcal{A}r^2} (r^2(T_1^{1(D)} + T_2^{2(D)} + 1) \\ & \left. \left. \left. + \mathcal{A}r^2 - \mathcal{B}^2 r^4 - 4\mathcal{B}r^2 - 1) \right) \right) \right], \quad (41) \end{aligned}$$

$$s^2 = \frac{r^2 e^{-\mathcal{A}r^2}}{2} \left( (\mathcal{B}r^2 + 1) \left( -\mathcal{A}r^2 + \mathcal{B}r^2 - 1 \right) + e^{\mathcal{A}r^2} \left( r^2(T_1^{1(D)} - T_2^{2(D)}) + 1 \right) \right). \quad (42)$$

The matching conditions can be used to evaluate the values of unknown constants  $\mathcal{B}$ ,  $\mathcal{C}$  and  $\mathcal{A}$ . The smooth matching between the external and internal geometries over the hypersurface assists in determining these constants. The continuum of the metric potentials between the outer and interior structures yields

$$\mathcal{B} = \frac{\mathbb{M}_o \mathbb{R} - \mathbb{S}_o^2}{\mathbb{R}^4 \left( -\frac{2\mathbb{M}_o}{\mathbb{R}} + \frac{\mathbb{S}_o^2}{\mathbb{R}^2} + 1 \right)}, \quad (43)$$

$$\mathcal{C} = \frac{\mathbb{R}^2 \left( -\frac{2\mathbb{M}_o}{\mathbb{R}} + \frac{\mathbb{S}_o^2}{\mathbb{R}^2} + 1 \right) \ln \left( -\frac{2\mathbb{M}_o}{\mathbb{R}} + \frac{\mathbb{S}_o^2}{\mathbb{R}^2} + 1 \right) - \mathbb{M}_o \mathbb{R} + \mathbb{S}_o^2}{\mathbb{R}^2 \left( -\frac{2\mathbb{M}_o}{\mathbb{R}} + \frac{\mathbb{S}_o^2}{\mathbb{R}^2} + 1 \right)}, \quad (44)$$

$$\mathcal{A} = \frac{1}{\mathbb{R}^2} \ln \left( \frac{1}{1 - \frac{2\mathbb{M}_o}{\mathbb{R}} + \frac{\mathbb{S}_o^2}{\mathbb{R}^2}} \right). \quad (45)$$

The anisotropic solutions of the internal compact structure is developed by using the radial and temporal metric components given in Eq.(39). Some new constraints can be employed to determine the solution of Eqs.(28)-(30) in which the anisotropic sector and geometric deformation function  $h^*$  are related. We consider the physical behavior of the compact star 4U 1820-30 [35] with radius and mass as  $9.1 \pm 0.4\text{km}$  and  $1.58 \pm 0.06M_\odot$ , respectively, which help to calculate the values of constant.

In the following, we study two anisotropic solutions.

## 4.1 Solution I

Here, we determine the deformation function  $h^*$  and constituents of extra source ( $\omega_\chi^\psi$ ) by taking an additional constraint at the radial part of the additional source. One can note that compatibility between inner source and outer Riessner-Nordström spacetime holds if  $\bar{P}(\mathbb{R}) - \frac{\mathbb{S}_o^2}{8\pi\mathbb{R}^4} + T_1^{1(D)}(\mathbb{R}) \sim \xi(\omega_1^1(\mathbb{R}))_-$ . This constraint is satisfied [21] when

$$\bar{P} - \frac{\mathbb{S}_o^2}{8\pi r^4} + T_1^{1(D)} = \omega_1^1, \quad (46)$$

yielding the deformation function  $h^*$  (using Eqs.(23) and (29)) as

$$h^* = \tau - \frac{1}{1 + \phi'r}. \quad (47)$$

The matching of the first fundamental form turns out to be

$$\mathbb{R}^2 e^{\mathcal{B}\mathbb{R}^2 + \mathcal{C}} = \mathbb{R}^2 - 2\mathbb{M}\mathbb{R} + \mathbb{S}^2, \quad (48)$$

$$\tau(1 + \beta) - \frac{\beta}{1 + 2\mathcal{C}\mathbb{R}^2} = 1 - \frac{2\mathbb{M}}{\mathbb{R}} + \frac{\mathbb{S}^2}{\mathbb{R}^2}. \quad (49)$$

In a similar way, the second fundamental form, i.e.,  $\bar{P}(\mathbb{R}) - \frac{\mathbb{S}_o^2}{8\pi\mathbb{R}^4} + T_1^{1(D)}(\mathbb{R}) - \xi(\omega_1^1(\mathbb{R}))_- = 0$  yields the constant  $\mathcal{A}$  through Eq.(46) as

$$\mathcal{A} = \frac{\ln(1 + 2\mathcal{B}\mathbb{R}^2)}{\mathbb{R}^2}. \quad (50)$$

Now, we extract the value of mass from Eqs.(33) and (49), and using in Eq.(48) provides the constant  $\mathcal{C}$  as

$$\mathcal{C} = \ln \left[ 1 - \frac{2\mathbb{M}_o}{\mathbb{R}} + \frac{\mathbb{S}_o^2}{\mathbb{R}^2} + \beta \left\{ 1 - \frac{2\mathbb{M}_o}{\mathbb{R}} + \frac{\mathbb{S}_o^2}{\mathbb{R}^2} - \frac{1}{1 + 2\mathcal{B}\mathbb{R}^2} \right\} \right] - \mathcal{B}\mathbb{R}^2. \quad (51)$$

Equations (50) and (51) are useful in matching the internal and external structures of the compact object. Applying the above mentioned constraints, we obtain  $\tilde{\mu}$ ,  $\tilde{P}_r$ ,  $\tilde{P}_t$  and  $s^2$  as

$$\begin{aligned} \tilde{\mu} = & \frac{e^{-\mathcal{A}r^2}}{32(\beta + 4\pi)(\beta + 8\pi)} \left[ \frac{1}{\pi(2\mathcal{B}r^3 + r)^2} \left\{ \xi(8\pi(r^4(-2\mathcal{A}^2(\mathcal{B}r^2 + 1) \right. \right. \\ & \times (2\mathcal{B}r^2 + 1) + \mathcal{A}\mathcal{B}(4\mathcal{B}r^2(\mathcal{B}r^2 + 8) + 27) - \mathcal{B}^2(14\mathcal{B}r^2 + 45)) \\ & + e^{\mathcal{A}r^2}(r^2(2\mathcal{B}(5r^2(T_1^{1(D)} + T_2^{2(D)})) + 3) + 3(T_1^{1(D)} + T_2^{2(D)})) + 1) \\ & - 1 + r^2(5\mathcal{A} - 18\mathcal{B})) + \beta(2\mathcal{B}r^6(\mathcal{A}^2 + 20\mathcal{A}\mathcal{B} - 7\mathcal{B}^2) + r^4(2\mathcal{A}^2 \\ & + 11\mathcal{A}\mathcal{B} - 65\mathcal{B}^2) + 4\mathcal{A}\mathcal{B}^2r^8(\mathcal{B} - \mathcal{A}) + e^{\mathcal{A}r^2}\mathcal{B}^2) + 4\mathcal{A}\mathcal{B}^2r^8(\mathcal{B} - \mathcal{A}) \\ & + e^{\mathcal{A}r^2}[(r^2(2\mathcal{B}(5r^2(T_0^{0(D)} + 2T_1^{1(D)} + T_2^{2(D)})) + 3) + 3(T_0^{0(D)} + 2T_1^{1(D)} \\ & + T_2^{2(D)})) + 1) - r^2(\mathcal{A} + 24\mathcal{B}) - 1)) \left. \right\} + \frac{8}{r^2} \left\{ \beta(\mathcal{B}r^4(\mathcal{A} - \mathcal{B}) + r^2(7\mathcal{A} \right. \\ & + 2\mathcal{B}) + e^{\mathcal{A}r^2}(r^2(-3T_0^{0(D)} - 2T_1^{1(D)} + T_2^{2(D)})) + 1) - 1) + 8\pi(\mathcal{B}r^4 \\ & \times (\mathcal{A} - \mathcal{B}) + e^{\mathcal{A}r^2}(r^2(-2T_0^{0(D)} - T_1^{1(D)} + T_2^{2(D)})) + 1) + 5\mathcal{A}r^2 - 1) \left. \right\} \right], \quad (52) \end{aligned}$$

$$\tilde{P}_r = \frac{1}{32\pi(\beta + 4\pi)(\beta + 8\pi)r^2} [(\xi + 8\pi)e^{-\mathcal{A}r^2}(\beta r^2(\mathcal{B}r^2(\mathcal{B} - \mathcal{A}) + \mathcal{A}$$

$$\begin{aligned}
& + 6\mathcal{B}) + 8\pi(\mathcal{B}r^4(\mathcal{B} - \mathcal{A}) - r^2(\mathcal{A} - 4\mathcal{B}) - e^{Ar^2}(r^2(T_1^{1(D)} + T_2^{2(D)})) + 1) \\
& + 1) - \beta e^{Ar^2}(r^2(T_0^{0(D)} + 2T_1^{1(D)} + T_2^{2(D)})) + 1) + \beta)], \tag{53}
\end{aligned}$$

$$\begin{aligned}
\tilde{P}_t = & \frac{1}{4(\beta + 4\pi)(\beta + 8\pi)(2\mathcal{B}r^2 + 1)^2} \left[ \xi e^{-Ar^2} (\mathcal{A}^2 r^2 (2\mathcal{B}^2 r^4 + 3\mathcal{B}r^2 + 1) \right. \\
& (\beta(\mathcal{B}r^2 - 1) + 8\pi(\mathcal{B}r^2 + 1)) - 2\mathcal{B}^3 r^4 (\beta r^2 + 1)) - 2\mathcal{B}^3 r^4 (\beta (e^{Ar^2} (r^2(T_0^{0(D)} \\
& + 2T_1^{1(D)} + T_2^{2(D)})) + 1) - 33) + 8\pi (e^{Ar^2} (r^2(T_1^{1(D)} + T_2^{2(D)})) + 1) - 24)) \\
& - \mathcal{B}^2 r^2 (\beta (e^{Ar^2} (9r^2(T_0^{0(D)} + 2T_1^{1(D)} + T_2^{2(D)})) + 7) - 51) + 8\pi (e^{Ar^2} (9r^2 \\
& \times (T_1^{1(D)} + T_2^{2(D)})) + 7) - 37)) - 2\mathcal{A}(\mathcal{B}\beta r^2 (2\mathcal{B}^3 r^6 + 12\mathcal{B}^2 r^4 + 11\mathcal{B}r^2 \\
& + 2) + 8\pi(2\mathcal{B}^4 r^8 + 12\mathcal{B}^3 r^6 + 17\mathcal{B}^2 r^4 + 8\mathcal{B}r^2 + 1)) - \mathcal{B}(\beta (e^{Ar^2} (7r^2(T_0^{0(D)} \\
& + 2T_1^{1(D)} + T_2^{2(D)})) + 4) - 10) + 8\pi (e^{Ar^2} (7r^2(T_1^{1(D)} + T_2^{2(D)})) + 4) - 8)) \\
& - e^{Ar^2} (\beta(T_0^{0(D)} + 2T_1^{1(D)} + T_2^{2(D)})) + 8\pi(T_1^{1(D)} + T_2^{2(D)})) + 2\mathcal{B}^5 (\beta + 8\pi)r^8 \\
& \left. + \mathcal{B}^4 (23\beta + 152\pi)r^6 \right] + \frac{1}{4(\beta + 4\pi)(\beta + 8\pi)r^2} \{ (e^{-Ar^2} (-\beta(\mathcal{A}\mathcal{B}r^4 + e^{Ar^2} \\
& \times (r^2(T_0^{0(D)} + 2T_1^{1(D)} + T_2^{2(D)})) + 1) - \mathcal{A}r^2 - \mathcal{B}^2 r^4 - 6\mathcal{B}r^2 - 1) - 8\pi(\mathcal{A}\mathcal{B}r^4 \\
& + e^{Ar^2} (r^2(T_1^{1(D)} + T_2^{2(D)})) + 1) + \mathcal{A}r^2 - \mathcal{B}^2 r^4 - 4\mathcal{B}r^2 - 1) \}, \tag{54}
\end{aligned}$$

$$\begin{aligned}
s^2 = & r^2 e^{-Ar^2} \left[ \frac{1}{4(\beta + 4\pi)(\beta + 8\pi)(2\mathcal{B}r^2 + 1)^2} \{ \xi (-8\pi\beta r^2 (\mathcal{B}(-2r^4(\mathcal{A}^2 \\
& + 11\mathcal{A}\mathcal{B} - 33\mathcal{B}^2) + 2\mathcal{B}^2 r^8 (\mathcal{A} - \mathcal{B})^2 + \mathcal{B}r^6 (\mathcal{A} - 23\mathcal{B})(\mathcal{A} - \mathcal{B}) + r^2 (51\mathcal{B} \\
& - 4\mathcal{A}) + 10) - \mathcal{A}^2 r^2) + 64\pi^2 r^2 (-\mathcal{A}^2 r^2 (2\mathcal{B}r^2 + 1) (\mathcal{B}r^2 + 1)^2 + 2\mathcal{A}(\mathcal{B}r^2 \\
& \times (2\mathcal{B}r^2 (\mathcal{B}r^2 + 5) + 7) + 1) (\mathcal{B}r^2 + 1) - \mathcal{B}(\mathcal{B}r^2 (\mathcal{B}r^2 (\mathcal{B}r^2 (2\mathcal{B}r^2 + 19) \\
& + 48) + 37) + 8)) + \beta (2\mathcal{B}r^2 + 1)^2 (\mathcal{B}r^4 (\mathcal{B} - \mathcal{A}) + r^2 (\mathcal{A} + 6\mathcal{B}) + 1) \\
& + 8\pi (2\mathcal{B}r^2 + 1)^2 (\mathcal{B}r^4 (\mathcal{B} - \mathcal{A}) - r^2 (\mathcal{A} - 4\mathcal{B}) + 1) + e^{Ar^2} (64\pi^2 (r^2 (2\mathcal{B}^3 \xi r^4 \\
& \times (r^2(T_1^{1(D)} + T_2^{2(D)})) + 1) + \mathcal{B}^2 r^2 (\xi (9r^2(T_1^{1(D)} + T_2^{2(D)})) + 7) + 24\beta r^2 (T_1^{1(D)} \\
& - T_2^{2(D)})) + 8) + \mathcal{B}(\xi (7r^2(T_1^{1(D)} + T_2^{2(D)})) + 4) + 24\beta r^2 (T_1^{1(D)} - T_2^{2(D)})) + 8) \\
& + \xi (T_1^{1(D)} + T_2^{2(D)})) + 6\beta (T_1^{1(D)} - T_2^{2(D)})) + 2) + 1024\pi^3 (2\mathcal{B}r^3 + r)^2 (T_1^{1(D)} \\
& - T_2^{2(D)}) + \beta (2\mathcal{B}r^2 + 1)^2 (4\beta + \xi (r^2 (-T_0^{0(D)} + 2T_1^{1(D)} + T_2^{2(D)})) - 1) \\
& + 8\pi (\xi \beta r^2 (\mathcal{B}(r^2 (2\mathcal{B}r^2 + 7) (\mathcal{B}(r^2 (T_0^{0(D)} + 2T_1^{1(D)} + T_2^{2(D)})) + 1) + T_0^{0(D)}
\end{aligned}$$

$$\begin{aligned}
& + 2T_1^{1(D)} + T_2^{2(D)}) + 4) + T_0^{0(D)} + 2T_1^{1(D)} + T_2^{2(D)}) - \xi(2\mathcal{B}r^2 + 1)^2(r^2(T_1^{1(D)} \\
& + T_2^{2(D)}) + 1) + 2\beta(2\mathcal{B}r^2 + 1)^2(2\beta r^2(T_1^{1(D)} - T_2^{2(D)} + 3))\}} + \mathcal{B}r^4(\mathcal{B} - \mathcal{A}) \\
& - \mathcal{A}r^2 - 1 \Big]. \tag{55}
\end{aligned}$$

## 4.2 Solution II

Now, we employ density like constraint ( $\bar{\mu} + \frac{s^2}{8\pi r^4} + T_0^{0(D)} = \omega_0^0$ ) to obtain the second anisotropic solution. Equations (22) and (28) along with this constraint yield

$$\frac{h^{\star'}}{r} + \frac{h^{\star}}{r^2} - \frac{1}{r^2} - \frac{e^{-\mathcal{A}r^2}}{r^2} + 2\mathcal{A}e^{-\mathcal{A}r^2} = 0, \tag{56}$$

whose integration gives the solution

$$h^{\star} = \frac{F_1}{r} + 1 - e^{-\mathcal{A}r^2}, \tag{57}$$

where  $F_1$  is the constant of integration. We choose  $F_1 = 0$  so that our resulting solution becomes free from any singularity at the core of the astrophysical object. In the current set up, the matching conditions are obtained by following the same procedure as in solution I

$$2\mathbf{R}(\mathbf{M} - \mathbf{M}_o) + \mathbf{S}_o^2 - \mathbf{S}^2 + \beta\mathbf{R}^2(1 - e^{-\mathcal{A}\mathbf{R}^2}) = 0, \tag{58}$$

$$C + \mathcal{B}\mathbf{R}^2 = \ln \left[ 1 - \frac{2\mathbf{M}_o}{\mathbf{R}} + \frac{\mathbf{S}_o^2}{\mathbf{R}^2} - \frac{\mathbf{S}^2}{\mathbf{R}^2} + \beta(1 - e^{-\mathcal{A}\mathbf{R}^2}) \right]. \tag{59}$$

The expressions for the state variables and charge are as follows

$$\begin{aligned}
\tilde{\mu} = & \frac{1}{32\pi(\beta + 4\pi)(\beta + 8\pi)r^2} \left[ (8\pi - \xi)e^{-\mathcal{A}r^2}(\beta(\mathcal{B}r^4(\mathcal{A} - \mathcal{B}) + r^2(7\mathcal{A} \right. \\
& + 2\mathcal{B}) + e^{\mathcal{A}r^2}(r^2(-3T_0^{0(D)} - 2T_1^{1(D)} + T_2^{2(D)} + 1) - 1) + 8\pi(\mathcal{B}r^4 \\
& \times (\mathcal{A} - \mathcal{B}) + e^{\mathcal{A}r^2}(r^2(-2T_0^{0(D)} - T_1^{1(D)} + T_2^{2(D)} + 1) + 5\mathcal{A}r^2 - 1)) \Big], \tag{60}
\end{aligned}$$

$$\tilde{P}_r = \frac{1}{768(\beta + 4\pi)(\beta + 8\pi)r^3} \left[ e^{-\mathcal{A}r^2} \left( \frac{1}{\pi\mathcal{A}^{5/2}} \{ \xi(2\mathcal{B}r^2 + 1)(3\sqrt{\pi}(\mathcal{A} + \mathcal{B}) \right. \right.$$

$$\begin{aligned}
& \times e^{Ar^2} (2\mathcal{A}(5\beta + 24\pi) - 3\mathcal{B}(\beta + 8\pi)) \text{Erf}(\sqrt{\mathcal{A}}r) - 2\sqrt{\mathcal{A}}r (2\mathcal{A}^2 (2e^{Ar^2} \\
& (2\mathcal{A}^2 (2e^{Ar^2} (\beta(r^2(3T_0^{0(D)} + 2T_1^{1(D)} - T_2^{2(D)}) - 3) + 8\pi(r^2(2T_0^{0(D)} + T_1^{1(D)} \\
& - T_2^{2(D)}) - 3)) + 3\beta(\mathcal{B}r^2 + 7) + 24\pi(\mathcal{B}r^2 + 5)) + 3\mathcal{A}\mathcal{B}(\beta(7 - 2\mathcal{B}r^2) \\
& + 8\pi(3 - 2\mathcal{B}r^2)) - 9\mathcal{B}^2(\beta + 8\pi))) \} + \{192r(\beta r^2(\mathcal{B}r^2(\mathcal{B} - \mathcal{A}) + \mathcal{A} + 6\mathcal{B}) \\
& + 8\pi(\mathcal{B}r^4(\mathcal{B} - \mathcal{A}) - r^2(\mathcal{A} - 4\mathcal{B}) - e^{Ar^2}(r^2(T_1^{1(D)} + T_2^{2(D)}) + 1) + 1) \\
& - \beta e^{Ar^2}(r^2(T_0^{0(D)} + 2T_1^{1(D)} + T_2^{2(D)}) + 1) + \beta) \} \Big], \tag{61}
\end{aligned}$$

$$\begin{aligned}
\tilde{P}_t = & \frac{1}{192(\beta + 4\pi)(\beta + 8\pi)r^3} \left[ e^{-Ar^2} \left( \frac{1}{\mathcal{A}^{5/2}} \{3\sqrt{\pi}\xi(\mathcal{A} + \mathcal{B})e^{Ar^2} (\mathcal{B}r^2(2\mathcal{B}r^2 \right. \right. \\
& + 3) - 1)(2\mathcal{A}(5\beta + 24\pi) - 3\mathcal{B}(\beta + 8\pi)) \text{Erf}(\sqrt{\mathcal{A}}r) \} + \frac{1}{\mathcal{A}^2} \{2r\} \} + \frac{1}{\mathcal{A}^2} \\
& \times \{2r(12\mathcal{A}^3 r^2 (\beta(\mathcal{B}r^2(\mathcal{B}\xi r^2 + 8\xi - 2) + 7\xi + 2) + 8\pi(\mathcal{B}r^2 + 1)(\mathcal{B}\xi r^2 \\
& + 5\xi - 2)) + 2\mathcal{A}^2 (-4\beta e^{Ar^2}(r^2(\xi(\mathcal{B}r^2(\mathcal{B}r^2 + 3) + 1)(3T_0^{0(D)} + 2T_1^{1(D)} \\
& - T_2^{2(D)}) + 3(-\mathcal{B}\xi(\mathcal{B}r^2 + 2) + 2T_1^{1(D)} + T_2^{2(D)}) + 3T_0^{0(D)}) + 3) + 8\pi \\
& \times (-4e^{Ar^2}(r^2(\xi(\mathcal{B}(r^2(\mathcal{B}(r^2(2T_0^{0(D)} + T_1^{1(D)} - T_2^{2(D)}) - 3) + 3(2T_0^{0(D)} \\
& + T_1^{1(D)} - T_2^{2(D)})) - 6) + 2T_0^{0(D)} + T_1^{1(D)} - T_2^{2(D)}) + 3(T_1^{1(D)} + T_2^{2(D)})) \\
& + 3) - 3\mathcal{B}r^2(\mathcal{B}r^2(4\mathcal{B}\xi r^2 + 15\xi - 4) + 16(\xi - 1)) + 9\xi + 12) + 3\beta(\mathcal{B}r^2 \\
& \times (\mathcal{B}r^2(-4\mathcal{B}\xi r^2 - 15\xi + 4) - 18\xi + 24) + 5\xi + 4) \} + 3\mathcal{A}\mathcal{B}\xi(\mathcal{B}r^2(2\mathcal{B}r^2 \\
& + 3) - 1)(\beta(2\mathcal{B}r^2 - 7) + 8\pi(2\mathcal{B}r^2 - 3)) + 9\mathcal{B}^2\xi(\beta + 8\pi)(\mathcal{B}r^2(2\mathcal{B}r^2 + 3) \\
& - 1)) \} \Big], \tag{62}
\end{aligned}$$

$$\begin{aligned}
s^2 = & \frac{1}{96\mathcal{A}^{5/2}(\beta + 4\pi)(\beta + 8\pi)} \left[ r^2 e^{-Ar^2} (-2\sqrt{\mathcal{A}}(48\mathcal{A}^3 r^2(\mathcal{B}r^2 + 1)(\pi\beta(\mathcal{B}\xi r^2 \right. \\
& + 7\xi + 12) + 8\pi^2(\mathcal{B}\xi r^2 + 5\xi + 4) + \beta^2) + 2\mathcal{A}^2(3(\beta(-8\mathcal{B}^2\beta r^4 + \xi(\mathcal{B}r^2 \\
& + 7)(2\mathcal{B}r^2 + 1) + 8\beta) - 4\pi\beta(\mathcal{B}r^2(\mathcal{B}r^2(4\mathcal{B}\xi r^2 + 15\xi + 24) + 18\xi) - 5\xi \\
& - 24) + 8\pi\xi(\mathcal{B}r^2 + 5)(2\mathcal{B}r^2 + 1) - 32\pi^2(\mathcal{B}r^2(\mathcal{B}r^2(4\mathcal{B}\xi r^2 + 15\xi + 8) \\
& + 16\xi) - 3\xi - 8)) - 2e^{Ar^2}(\beta(\xi(-2\mathcal{B}r^2 - 1)(r^2(3T_0^{0(D)} + 2T_1^{1(D)} - T_2^{2(D)}) \\
& - 3) + 12\beta) + 64\pi^2(r^2(\xi(\mathcal{B}(r^2(\mathcal{B}(r^2(2T_0^{0(D)} + T_1^{1(D)} - T_2^{2(D)}) - 3) + 3 \\
& \times (2T_0^{0(D)} + T_1^{1(D)} - T_2^{2(D)})) - 6) + 2T_0^{0(D)} + T_1^{1(D)} - T_2^{2(D)}) + 18\beta(T_1^{1(D)}
\end{aligned}$$

$$\begin{aligned}
& - T_2^{2(D)}) + 6) + 8\pi(\xi\beta r^2(\mathcal{B}(r^2(\mathcal{B}(r^2(3T_0^{0(D)} + 2T_1^{1(D)} - T_2^{2(D)})) - 3) \\
& + 9T_0^{0(D)} + 6T_1^{1(D)} - 3T_2^{2(D)}) - 6) + 3T_0^{0(D)} + 2T_1^{1(D)} - T_2^{2(D)}) + \xi(-2\mathcal{B}r^2 \\
& - 1)(r^2(2T_0^{0(D)} + T_1^{1(D)} - T_2^{2(D)}) - 3) + 6\beta(2\beta r^2(T_1^{1(D)} - T_2^{2(D)}) + 3)) \\
& + 3072\pi^3 r^2(T_1^{1(D)} - T_2^{2(D)})) + 3\mathcal{A}\mathcal{B}\xi(8\pi\mathcal{B}^2 r^4 + 2(6\pi - 1)\mathcal{B}r^2 - 4\pi - 1) \\
& \times (\beta(2\mathcal{B}r^2 - 7) + 8\pi(2\mathcal{B}r^2 - 3)) + 9\mathcal{B}^2\xi(\beta + 8\pi)(8\pi\mathcal{B}^2 r^4 + 2(6\pi - 1)\mathcal{B}r^2 \\
& - 4\pi - 1)) - \frac{1}{r}\{3\sqrt{\pi}\xi(\mathcal{A} + \mathcal{B})e^{Ar^2}(8\pi\mathcal{B}^2 r^4 + 2(6\pi - 1)\mathcal{B}r^2 - 4\pi - 1) \\
& \times (2\mathcal{A}(5\beta + 24\pi) - 3\mathcal{B}(\beta + 8\pi))\text{Erf}(\sqrt{Ar})\}\}. \tag{63}
\end{aligned}$$

## 5 Physical Aspects

In this section, we examine physical viability and stability of the resulting solutions. The anisotropy for the solution I becomes

$$\begin{aligned}
\tilde{\Delta} &= \frac{\xi e^{-Ar^2}}{32(\beta + 4\pi)(\beta + 8\pi)} \left[ \frac{8}{(2\mathcal{B}r^2 + 1)^2} \{ (\mathcal{A}^2 r^2 (\mathcal{B}r^2 + 1) (2\mathcal{B}r^2 + 1) (\beta (\mathcal{B}r^2 \right. \\
& - 1) + 8\pi (\mathcal{B}r^2 + 1)) - 2\mathcal{A}\mathcal{B}\beta r^2 (\mathcal{B}r^2 (2\mathcal{B}r^2 (\mathcal{B}r^2 + 6) + 11) + 2) - e^{Ar^2} (\beta \\
& \times (\mathcal{B}(r^2 (2\mathcal{B}r^2 + 7) (\mathcal{B}(r^2 (T_0^{0(D)} + 2T_1^{1(D)} + T_2^{2(D)})) + 1) + T_0^{0(D)} + 2T_1^{1(D)} \\
& + T_2^{2(D)}) + 4) + T_0^{0(D)} + 2T_1^{1(D)} + T_2^{2(D)}) + 8\pi (\mathcal{B}(r^2 (2\mathcal{B}r^2 + 7) (\mathcal{B}(r^2 (T_1^{1(D)} \\
& + T_2^{2(D)})) + 1) + T_1^{1(D)} + T_2^{2(D)}) + 4) + T_1^{1(D)} + T_2^{2(D)})) - 16\pi\mathcal{A}(\mathcal{B}r^2 + 1) \\
& \times (\mathcal{B}r^2 (2\mathcal{B}r^2 (\mathcal{B}r^2 + 5) + 7) + 1) + 2\mathcal{B}^5\beta r^8 + 16\pi\mathcal{B}^5 r^8 + 23\mathcal{B}^4\beta r^6 + 152 \\
& \times \pi\mathcal{B}^4 r^6 + 66\mathcal{B}^3\beta r^4 + 384\pi\mathcal{B}^3 r^4 + 51\mathcal{B}^2\beta r^2 + 296\pi\mathcal{B}^2 r^2 + 10\mathcal{B}\beta + 64\pi\mathcal{B}) \} \\
& + \frac{1}{\pi r^2} \{ \beta (\mathcal{B}r^4 (\mathcal{A} - \mathcal{B}) - r^2 (\mathcal{A} + 6\mathcal{B}) + e^{Ar^2} (r^2 (T_0^{0(D)} + 2T_1^{1(D)} + T_2^{2(D)})) + 1) \\
& - 1) + 8\pi (\mathcal{B}r^4 (\mathcal{A} - \mathcal{B}) + r^2 (\mathcal{A} - 4\mathcal{B}) + e^{Ar^2} (r^2 (T_1^{1(D)} + T_2^{2(D)})) + 1) - 1) \} \Big], \tag{64}
\end{aligned}$$

whereas for solution II, we have

$$\begin{aligned}
\tilde{\Delta} &= \frac{e^{-Ar^2}}{768(\beta + 4\pi)(\beta + 8\pi)r^3} \left[ \frac{1}{\sqrt{\pi}\mathcal{A}^{5/2}} \{ 3\xi(\mathcal{A} + \mathcal{B})e^{Ar^2}(8\pi\mathcal{B}^2 r^4 + 2(6\pi - 1)\mathcal{B}r^2 \right. \\
& - 4\pi - 1)(2\mathcal{A}(5\beta + 24\pi) - 3\mathcal{B}(\beta + 8\pi))\text{Erf}(\sqrt{Ar}) \} + \frac{2\xi r}{\pi\mathcal{A}^2} \{ (48\pi\mathcal{A}^3 r^2 (\mathcal{B}r^2
\end{aligned}$$

$$\begin{aligned}
& + 1)(\beta(\mathcal{B}r^2 + 7) + 8\pi(\mathcal{B}r^2 + 5)) + 2\mathcal{A}^2(\beta(2\mathcal{B}r^2 + 1)(e^{Ar^2}(r^2(6T_0^{0(D)} + 4T_1^{1(D)} \\
& - 2T_2^{2(D)}) - 6) + 3(\mathcal{B}r^2 + 7)) + 4\pi(-4e^{Ar^2}(\beta r^2(\mathcal{B}(r^2(\mathcal{B}(r^2(3T_0^{0(D)} + 2T_1^{1(D)} \\
& - T_2^{2(D)}) - 3) + 9T_0^{0(D)} + 6T_1^{1(D)} - 3T_2^{2(D)}) - 6) + 3T_0^{0(D)} + 2T_1^{1(D)} - T_2^{2(D)}) \\
& + (-2\mathcal{B}r^2 - 1)(r^2(2T_0^{0(D)} + T_1^{1(D)} - T_2^{2(D)}) - 3)) - 3\mathcal{B}r^2(\mathcal{B}r^2(4\mathcal{B}\beta r^2 + 15\beta \\
& - 4) + 18\beta - 22) + 15(\beta + 2)) + 32\pi^2(r^2(-4e^{Ar^2}(\mathcal{B}(r^2(\mathcal{B}(r^2(2T_0^{0(D)} + T_1^{1(D)} \\
& - T_2^{2(D)}) - 3) + 3(2T_0^{0(D)} + T_1^{1(D)} - T_2^{2(D)})) - 6) + 2T_0^{0(D)} + T_1^{1(D)} - T_2^{2(D)}) \\
& - 3\mathcal{B}(\mathcal{B}r^2(4\mathcal{B}r^2 + 15) + 16)) + 9)) + 3\mathcal{A}\mathcal{B}(8\pi\mathcal{B}^2r^4 + 2(6\pi - 1)\mathcal{B}r^2 - 4\pi \\
& - 1)(\beta(2\mathcal{B}r^2 - 7) + 8\pi(2\mathcal{B}r^2 - 3)) + 9\mathcal{B}^2(\beta + 8\pi)(8\pi\mathcal{B}^2r^4 + 2(6\pi - 1)\mathcal{B}r^2 \\
& - 4\pi - 1))\}}]. \tag{65}
\end{aligned}$$

It is well-known that the anisotropic factor shows positive behavior if  $\tilde{P}_t > \tilde{P}_r$ , indicating that the anisotropic force is acting outward. When  $\tilde{P}_r > \tilde{P}_t$ , the anisotropy is negative and squeezes the matter within the star (together with gravitational force).

In order to observe the physical analysis of the obtained solutions, we consider the model (7) with parameter  $\beta$  as 0.01 and charge parameter (s) as 0.1 and 0.9. The value of the constant  $\mathcal{A}$  is taken from (50) while  $\mathcal{B}$  as well as  $\mathcal{C}$  are fixed from (43) and (44). The effective matter determinants ( $\tilde{\mu}, \tilde{P}_r, \tilde{P}_t$ ) must be positive, maximum and finite in the inner structure of the charged celestial object or we can say that these parameters should decrease as  $r$  increases. Figure 1 shows that  $\tilde{\mu}, \tilde{P}_r$  and  $\tilde{P}_t$  for solution I decrease monotonically towards the boundary as  $r$  increases. Also, it is observed that the effective density of the system decreases with charge showing that the stellar object becomes less dense for larger charge while the radial/tangential pressures become zero at the boundary. The last plot of Figure 1 demonstrates that anisotropy decreases with  $r$  but increases with  $\xi$  in the current set up. Thus, one can observe that anisotropy is positive, meaning that it will act in the outward direction of the star. The higher values of the decoupling parameter  $\xi$  assures more anisotropic system.

The compactness parameter (ratio between star's mass and radius) is considered as an important aspect of self-gravitating stellar objects. Buchdahl [36] matched the Schwarzschild exterior vacuum region with the interior spherical geometry to evaluate the upper limit of compactness parameter as  $\frac{m}{R} < \frac{4}{9}$ , where  $m = \frac{R}{2}(1 - e^{-\lambda})$ . However, the Buchdahl limit (upper bound)

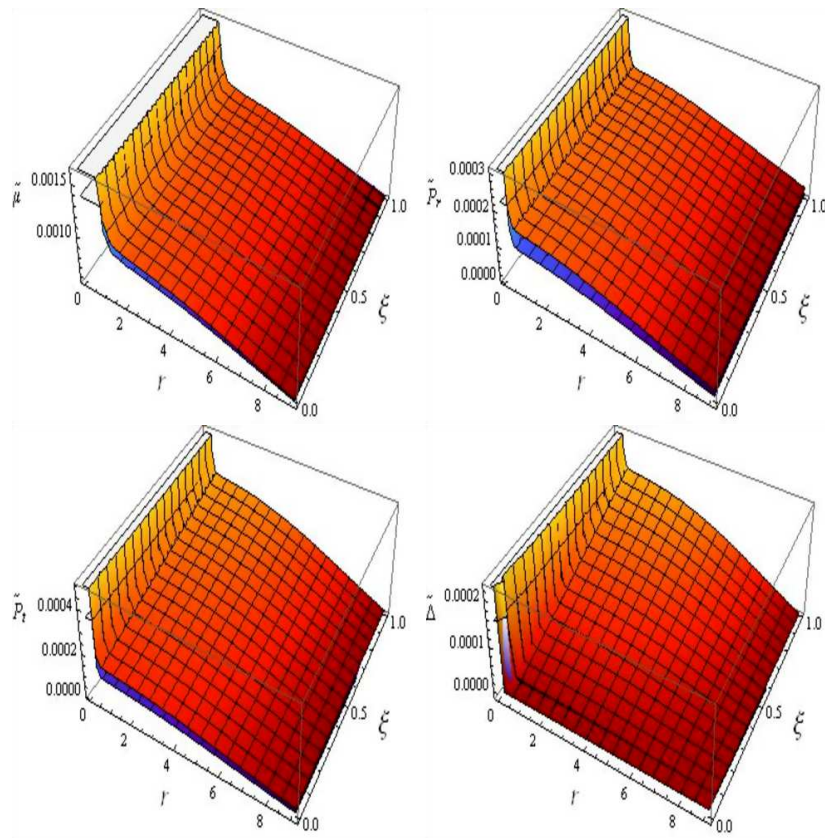


Figure 1: Plots of  $\tilde{\mu}, \tilde{P}_r, \tilde{P}_t$  and  $\tilde{\Delta}$  versus  $r$  and  $\xi$  with  $S_o = 0.1$  (Orange),  $S_o = 0.9$  (Blue) for the solution I.

has been modified due to the involvement of charge in the matter source. The upper bound of mass-radius ratio is modified by Andreasson [37] for a charged spherical astrophysical object and is defined as  $\zeta(r) = \frac{m}{R} < \frac{2}{9} + \frac{3S_o^2 + 2R\sqrt{R^2 + 3S_o^2}}{9R^2}$ . The mass of the static spherical celestial object can be determined by

$$m = 4\pi \int_0^R \left( \tilde{\mu} + \frac{S^2}{8\pi r^4} \right) r^2 dr. \quad (66)$$

The numerical technique is employed to determine the mass of anisotropic structure along with the initial condition  $m(0) = 0$ . The wavelength of the electromagnetic radiations produced by a celestial object, having a strong gravitational force, increases. This increment is calculated by the redshift factor whose mathematical expression is  $Z(r) = \frac{1}{\sqrt{1-2\zeta}} - 1$ . For perfect matter source, Buchdahl restricted this parameter to  $Z(r) < 2$  at the star's surface while for the anisotropic configurations, this value is observed as 5.211 [38]. Another important quantity of self-gravitating objects is the equation of state (EoS) parameter, defined as

$$\tilde{\mathbf{w}}_r = \frac{\tilde{P}_r}{\tilde{\mu}}, \quad \tilde{\mathbf{w}}_t = \frac{\tilde{P}_t}{\tilde{\mu}}. \quad (67)$$

For the effectiveness of the stellar matter source, both the EoS parameters (radial and tangential) must lie in [0,1] [39].

Stability is another important factor in the analysis of compact objects. There are various methods to check the stability of the celestial objects like Herrera cracking approach and causality condition. According to Herrera cracking approach [40], the velocity of the considered system must satisfy  $|\nu_t^2 - \nu_r^2| < 1$ , where  $\nu_r^2$  and  $\nu_t^2$  are the squared speed sound in radial and tangential directions given as  $\nu_r^2 = \frac{dP_r}{d\mu}$  and  $\nu_t^2 = \frac{dP_t}{d\mu}$ , respectively. The causality condition states that the speed of sound should be less than the speed of light and its components must lie in the interval 0 and 1, i.e.,  $0 < \nu_t^2 < 1$  and  $0 < \nu_r^2 < 1$ .

The fluid distribution of a stellar body is characterized by EMT on which some limitations are enforced called as energy conditions. The viability of the obtained solutions as well as the existence of normal matter are checked using these conditions. It is also important that the parameters governing the internal structure must satisfy these conditions. These limitations are divided as dominant, weak, null and strong energy conditions. In  $f(G, T)$

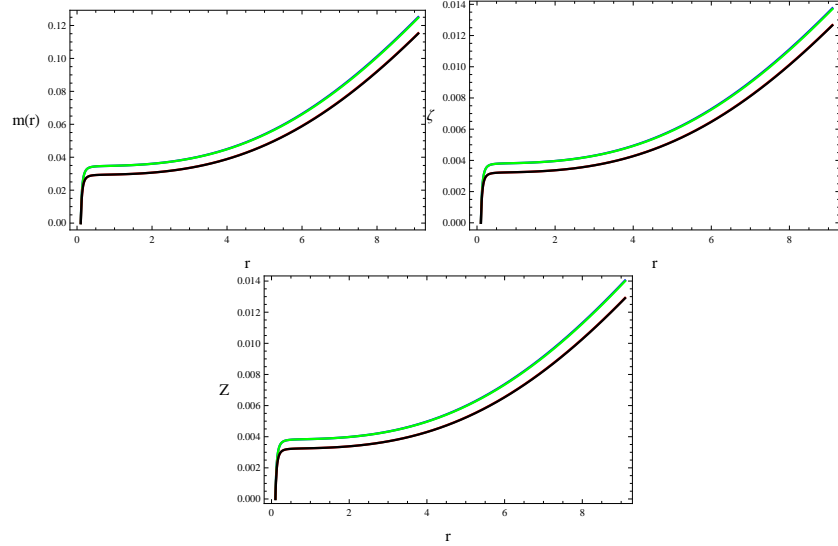


Figure 2: Plots of mass, compactness and redshift versus  $r$  corresponding to  $\mathbb{S}_o = 0.1$ ,  $\xi = 0.01$  (Blue),  $\xi = 0.9$  (Green) and  $\mathbb{S}_o = 0.9$ ,  $\xi = 0.01$  (Red),  $\xi = 0.9$  (Black) for solution I.

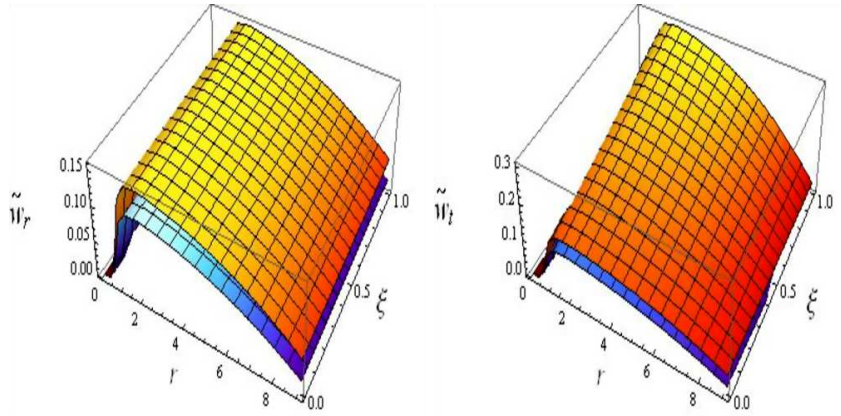


Figure 3: Plots of EoS parameters versus  $r$  and  $\xi$  with  $\mathbb{S}_o = 0.1$  (Orange),  $\mathbb{S}_o = 0.9$  (Blue) for the solution I.

theory, these constraints are described as

$$\begin{aligned}
\tilde{\mu} + \frac{s^2}{8\pi r^4} &\geq 0, & \tilde{\mu} + \tilde{P}_r &\geq 0, \\
\tilde{\mu} + \tilde{P}_t + \frac{s^2}{4\pi r^4} &\geq 0, & \tilde{\mu} - \tilde{P}_r + \frac{s^2}{4\pi r^4} &\geq 0, \\
\tilde{\mu} - \tilde{P}_t &\geq 0, & \tilde{\mu} + \tilde{P}_r + 2\tilde{P}_t + \frac{s^2}{4\pi r^4} &\geq 0.
\end{aligned} \tag{68}$$

For mass, compactness and redshift parameter, we use distinct values of the decoupling parameter along with charge. Figure 2 (1st plot) illustrates that the mass function decreases for an increasing charge. Figure 2 (2nd and 3rd plots) and Figure 3 indicate that the compactness as well as redshift parameters and the EoS parameters, respectively, lie within the required limit. The energy conditions (68) for the solution I are satisfied as shown in Figure 4 which indicates physical viability of the solution. Figure 5 shows that the first solution fulfills both the stability criterion, hence the solution I is stable. The graphical analysis of the solution II is given for the same values of the decoupling parameter and charge as for the solution I. The constant terms  $\mathcal{A}$  and  $\mathcal{B}$  are taken from Eqs.(45) and (59). The effective energy density, radial as well as tangential pressures of the second solution exhibit the decreasing behavior with increase in  $r$  (Figure 6) but for the larger charge, the effective energy density of the star decreases. Figure 6 demonstrates that the anisotropy increases with the decoupling parameter. Figure 7 shows mass, compactness and redshift parameter meet their desired ranges. Moreover, these factors decrease for higher  $\xi$  and charge. Likewise, the EoS parameters for the second solution meet the required limits (Figure 8). Figure 9 shows that all the energy conditions are satisfied ensuring the viability of the system. The radial component of the sound velocity obeys the stability criterion (Figure 10) whereas the tangential component shows unstable behavior at the core but becomes stable for larger values of the decoupling parameter. However, according to cracking approach, the second solution shows consistent behavior.

## 6 Conclusions

Astrophysicists have made various efforts in developing physically viable and stable solutions for compact objects. A recently developed technique

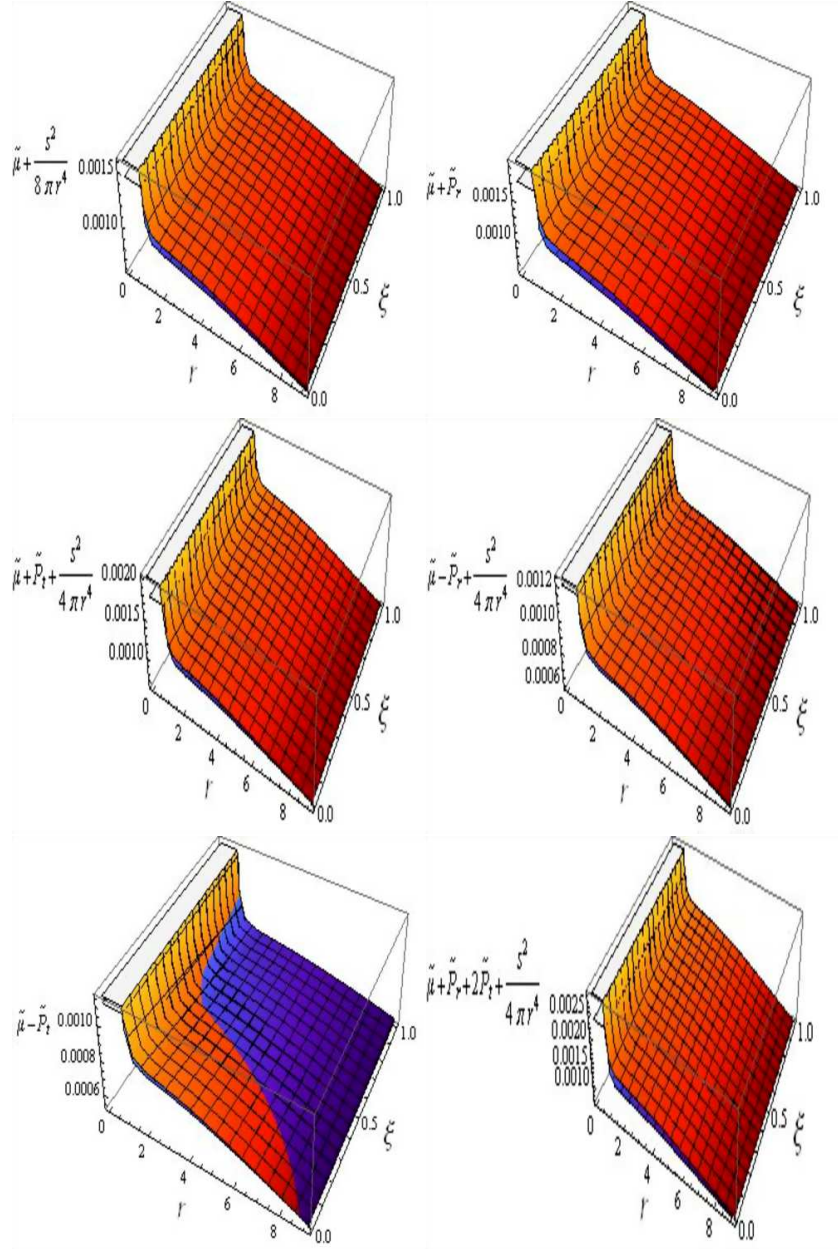


Figure 4: Plots of energy conditions versus  $r$  and  $\xi$  with  $\mathbb{S}_o = 0.1$  (Orange),  $\mathbb{S}_o = 0.9$  (Blue) for the solution I.

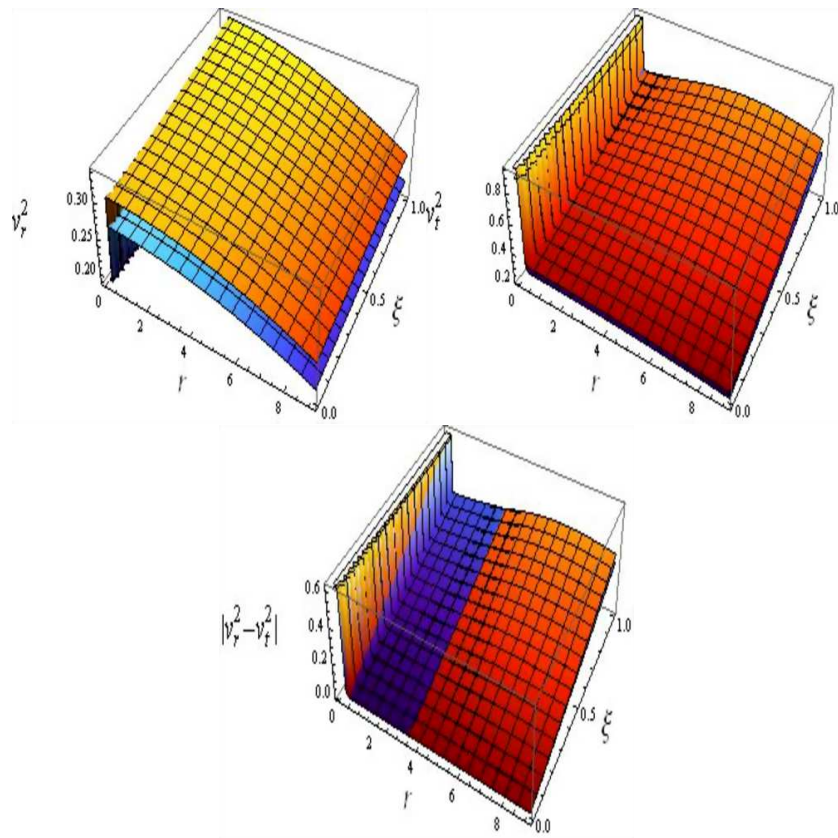


Figure 5: Plots of causality condition and Herrera cracking approach versus  $r$  and  $\xi$  with  $S_o = 0.1$  (Orange),  $S_o = 0.9$  (Blue) for the solution I.

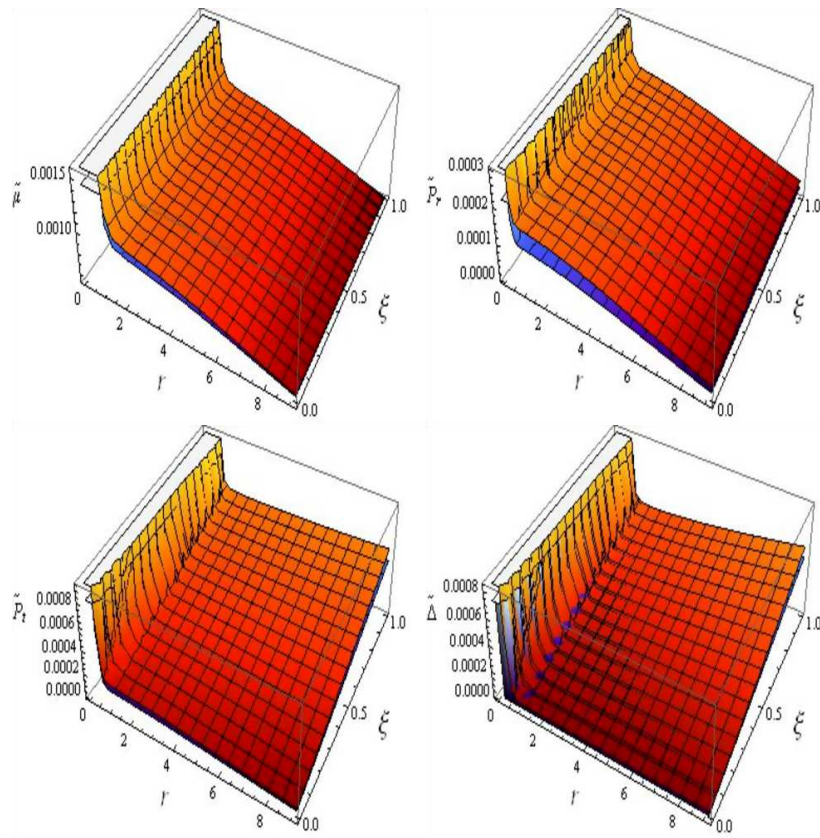


Figure 6: Plots of  $\tilde{\mu}, \tilde{P}_r, \tilde{P}_t$  and  $\tilde{\Delta}$  versus  $r$  and  $\xi$  with  $S_o = 0.1$  (Orange),  $S_o = 0.9$  (Blue) for the solution II.

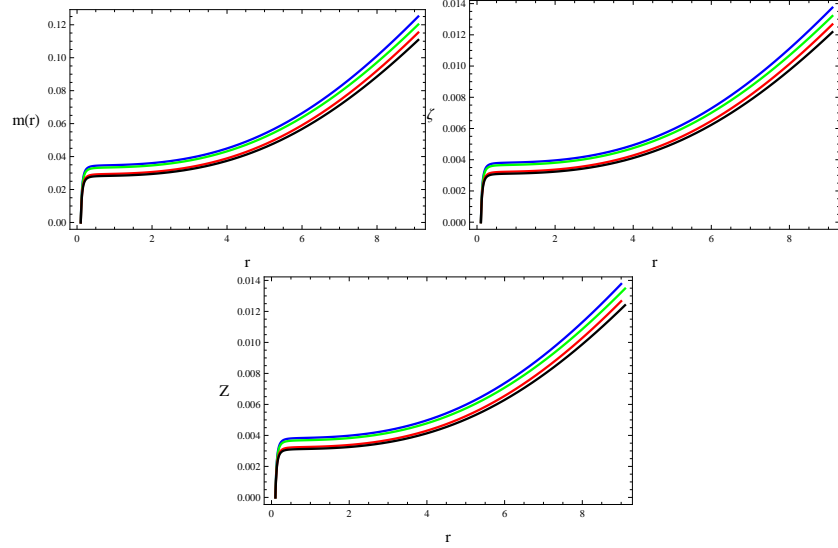


Figure 7: Plots of mass, compactness and redshift versus  $r$  corresponding to  $\mathbb{S}_o = 0.1$ ,  $\xi = 0.01$  (Blue),  $\xi = 0.9$  (Green) and  $\mathbb{S}_o = 0.9$ ,  $\xi = 0.01$  (Red),  $\xi = 0.9$  (Black) for solution II.

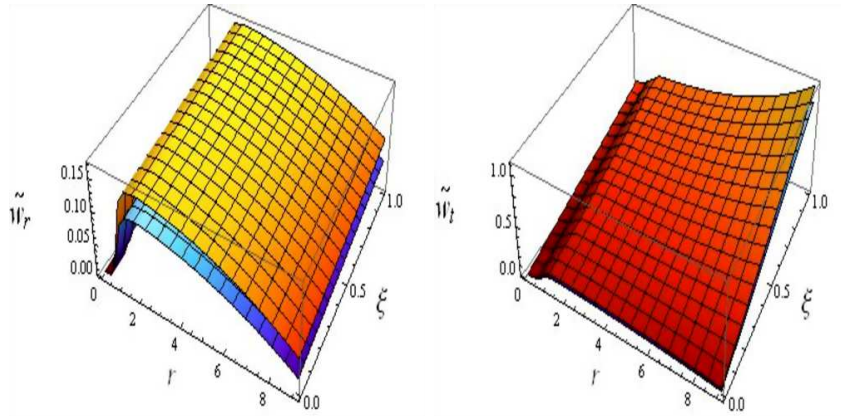


Figure 8: Plots of EoS parameters versus  $r$  and  $\xi$  with  $\mathbb{S}_o = 0.1$  (Orange),  $\mathbb{S}_o = 0.9$  (Blue) for the solution II.

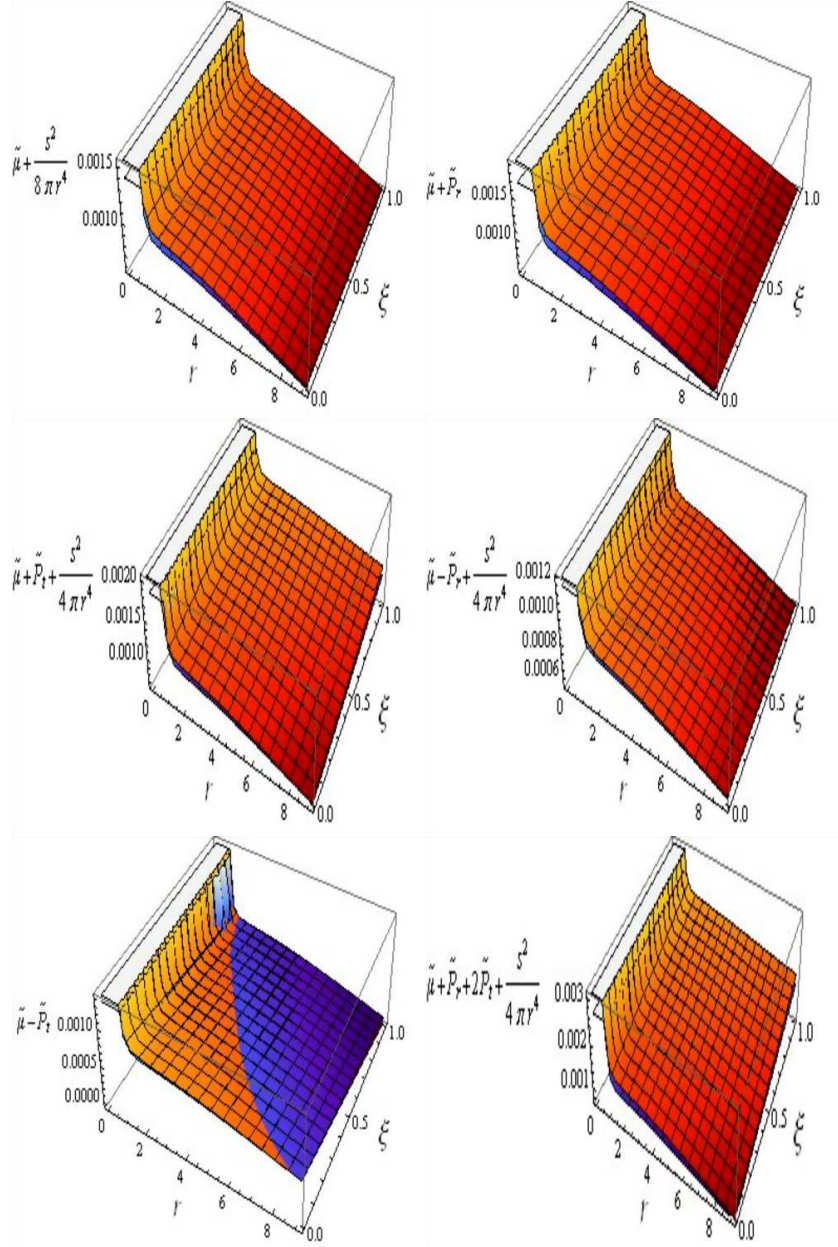


Figure 9: Plots of energy conditions versus  $r$  and  $\xi$  with  $\mathbb{S}_o = 0.1$  (Orange),  $\mathbb{S}_o = 0.9$  (Blue) for the solution II.

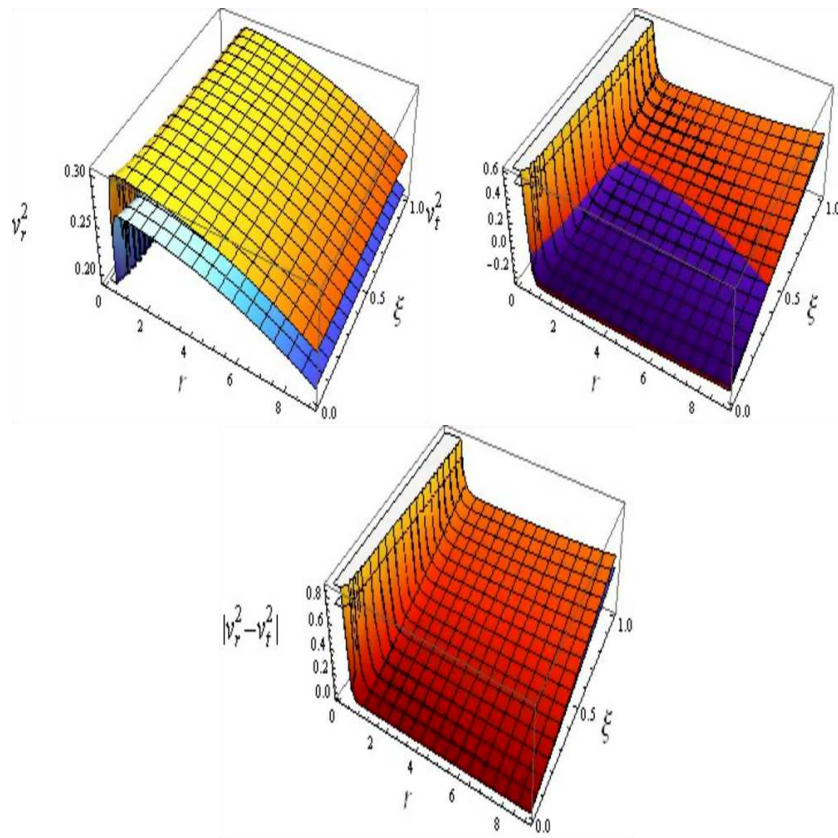


Figure 10: Plots of causality condition and Herrera cracking approach versus  $r$  and  $\xi$  with  $S_o = 0.1$  (Orange),  $S_o = 0.9$  (Blue) for the solution II.

termed as gravitational decoupling through MGD has been found useful to understand the internal configurations of the stellar structures through their anisotropic solutions. In this paper, we have used this method to evaluate anisotropic solutions for  $f(G, T) = G^2 + \beta T$  gravity model with charged spherically symmetric geometry. The charged isotropic static sphere is filled with the new source to induce anisotropy in it. This scheme basically deforms the field equations into two sets representing the isotropic and anisotropic systems. We have considered the Krori-Barua ansatz to solve the system related to isotropic source in which the values of unknowns are extracted through junction conditions. For the second set (28)-(30), we have employed some extra constraints on  $\omega_{\psi\chi}$  to evaluate the unknown quantities. Finally, we have checked viable and stable behavior of the obtained anisotropic solutions through graphical analysis.

We have investigated physical properties of the effective state variables  $(\tilde{\mu}, \tilde{P}_r, \tilde{P}_t)$ , anisotropy  $(\tilde{\Delta})$  and energy conditions (68) with  $\beta = 0.01$  to check physical viability of the developed solutions. It is found that our both solutions satisfy the required limits for mass, compactness, redshift as well as EoS parameters. For both solutions, the self-gravitating object becomes less dense as charge increases. Both solutions satisfy all the energy conditions, hence they are physically viable. We have found that both the stability criteria are satisfied for the first solution, while the second solution is shown consistent only with the cracking approach. Solution II shows stable behavior for higher values of the decoupling parameter with causality condition. It is mentioned here that two anisotropic solutions were found in GR [23], one was viable but unstable, while the other was neither viable nor stable. However, in  $f(G)$  gravity all the developed solutions were well-behaved [29]. Here we have found that this theory provides more better solutions than GR but similar to  $f(G)$  gravity. It is worth mentioning here that our results reduce to GR for  $f(G, T) = 0$ .

## Appendix A

The values of Gauss-Bonnet invariant and its derivatives are given as

$$\begin{aligned}
 G &= \frac{1}{r^2} \left[ 2e^{-2\lambda} \left( (e^\lambda - 3) \phi' \lambda' - (e^\lambda - 1) (2\lambda'' + \phi'^2) \right) \right], \\
 G' &= \frac{-1}{r^3} \left[ 2e^{-2\lambda} \left( -r\phi' \left( (e^\lambda - 3) \lambda'' - 2(e^\lambda - 1) \phi'' \right) + r(e^\lambda - 6) \phi' \lambda'^2 \right) \right],
 \end{aligned} \tag{A1}$$

$$\begin{aligned}
& + \lambda' \left( -r (3e^\lambda - 7) \phi'' + r (- (e^\lambda - 2)) \phi'^2 + 2 (e^\lambda - 3) \phi' r \right) - 2 (e^\lambda \\
& - 1) \phi'^2 - 2 (e^\lambda - 1) (2\phi'' - r\phi^{(3)}) \Big], \tag{A2}
\end{aligned}$$

$$\begin{aligned}
G'' & = \frac{1}{r^4} \left[ 2e^{-2\lambda} \left( \phi'^2 (r^2 (e^\lambda - 2) \lambda'' - 6e^\lambda + 6) - 2 \left( \phi'' (6(e^\lambda - 1) - r^2 (2e^\lambda \right. \right. \right. \\
& - 5) \lambda'' \left. \left. \left. + r^2 (e^\lambda - 1) \phi''^2 + r (r\phi^{(4)} - 4\phi^{(3)}) (e^\lambda - 1) \right) \right) + r^2 (e^\lambda - 12) \right. \\
& \times \phi' \lambda'^3 + \lambda' \left( \phi' (-3r^2 (e^\lambda - 6) \lambda'' + 4r^2 (e^\lambda - 2) \phi'' + 6(e^\lambda - 3)) - 4 \right. \\
& \times r (e^\lambda - 2) \phi'^2 + r (r\phi^{(3)} (5e^\lambda - 11) - 4(3e^\lambda - 7) \phi'') \left. \right) - r \lambda'^2 \left( 4r (e^\lambda \right. \\
& - 5) \phi'' + r (e^\lambda - 4) \phi'^2 - 4(e^\lambda - 6) \phi' \left. \right) + r \phi' \left( r ((e^\lambda - 3) \lambda^{(3)} - 2\phi^{(3)} \right. \\
& \times (e^\lambda - 1)) - 4(e^\lambda - 3) \lambda'' + 8(e^\lambda - 1) \phi'' \left. \right) \Big]. \tag{A3}
\end{aligned}$$

The correction terms corresponding to  $f(G, T)$  gravity become

$$\begin{aligned}
T_0^{0(D)} & = \frac{1}{8\pi} \left[ -\frac{1}{2} \zeta G^2 + \left( \frac{4e^{-2\lambda} \phi''}{r^2} - \frac{4e^{-\lambda} \phi''}{r^2} - \frac{2e^{-\lambda} \phi'^2}{r^2} + \frac{2e^{-\lambda} \phi' \lambda'}{r^2} \right. \right. \\
& + \left. \frac{2e^{-2\lambda} \phi'^2}{r^2} - \frac{6e^{-2\lambda} \phi' \lambda'}{r^2} \right) G + \left( \frac{12e^{-2\lambda} \lambda'}{r^2} - \frac{4e^{-\lambda} \lambda'}{r^2} \right) G' \\
& \left. \left( -\frac{8e^{-2\lambda}}{r^2} + \frac{8e^{-\lambda}}{r^2} \right) G'' \right], \tag{A4}
\end{aligned}$$

$$\begin{aligned}
T_1^{1(D)} & = \frac{1}{8\pi} \left[ \frac{1}{2} \zeta G^2 + \left( -\frac{4e^{-2\lambda} \phi''}{r^2} + \frac{4e^{-\lambda} \phi''}{r^2} + \frac{6e^{-2\lambda} \phi' \lambda'}{r^2} - \frac{2e^{-\lambda} \phi' \lambda'}{r^2} \right. \right. \\
& - \left. \frac{2e^{-2\lambda} \phi'^2}{r^2} + \frac{2e^{-\lambda} \phi'^2}{r^2} \right) G + \left( \frac{12e^{-2\lambda} \phi'}{r^2} - \frac{4e^{-\lambda} \phi'}{r^2} \right) G' \Big], \tag{A5}
\end{aligned}$$

$$T_2^{2(D)} = \frac{1}{8\pi} \left[ \frac{1}{2} G^2 + \left( -\frac{4e^{-2\lambda} \phi''}{r^2} + \frac{4e^{-\lambda} \phi''}{r^2} + \frac{2e^{-\lambda} \phi'^2}{r^2} - \frac{2e^{-2\lambda} \phi'^2}{r^2} \right) \right]$$

$$\begin{aligned}
& - \frac{2e^{-\lambda}\phi'\lambda'}{r^2} + \frac{6e^{-2\lambda}\phi'\lambda'}{r^2} \Big) G + \left( - \frac{6e^{-2\lambda}\phi'\lambda'}{r} + \frac{4e^{-2\lambda}\phi''}{r} \right. \\
& \left. + \frac{2e^{-2\lambda}\phi'^2}{r} \right) G' + \frac{4e^{-2\lambda}\phi'}{r} G'' \Big]. \tag{A6}
\end{aligned}$$

The term  $\Omega$  comes out to be

$$\Omega = \frac{\beta}{8\pi - \beta} \left[ - \frac{(-\mu + 3P + \xi\omega)'}{2} - \xi\omega_1^1 (\ln f_T)' + (-2P - 2\xi\omega_1^1)' - \frac{ss'}{4\pi r^4} \right]. \tag{A7}$$

## Data Availability Statement

This manuscript has no associated data.

## References

- [1] Van Albada, T.S. and Sancisi, R.: *Philos. Trans. Royal Soc. A* **320**(1986)447; Swaters, R.A., Madore, B.F. and Trewhella, M.: *Astrophys. J.* **531**(2000)L107.
- [2] Barrow, J.D., Maartens, R. and Tsagas, C.G.: *Phys. Rep.* **449**(2007)131; Neveu, J. et al.: *Astron. Astrophys.* **600**(2017)A40.
- [3] Lovelock, D.: *J. Math. Phys.* **12**(1971)498.
- [4] Nojiri, S. and Odintsov, S.D.: *Phys. Lett. B* **631**(2005)1.
- [5] Sharif, M. and Ikram, A.: *Eur. Phys. J. C* **76**(2016)640.
- [6] Sharif, M. and Ikram, A.: *Int. J. Mod. Phys. D* **27**(2018)1750182.
- [7] Yousaf, Z., Bhatti, M.Z. and Hassan, K.: *Eur. Phys. J. Plus* **135**(2020)397; Yousaf, Z. et al.: *New Astron.* **84**(2021)101541.
- [8] Sharif, M. and Hassan, K.: *Chin. J. Phys* **77**(2022)1479; *Pramana* **96**(2022)50; *Mod. Phys. Lett. A* **37**(2022)2250027.
- [9] Xingxiang, W.: *Gen. Relativ. Gravit.* **19**(1978)729.
- [10] Das, B. et al.: *Int. J. Mod. Phys. D* **20**(2011)1675.

- [11] Sharif, M. and Bhatti, M.Z.: *Astrophys. Space Sci.* **347**(2013)337.
- [12] Murad, M.H.: *Astrophys. Space Sci.* **361**(2016)20.
- [13] Singh, K.N. and Pant, N.: *Astrophys. Space Sci.* **358**(2015)1; Sharif, M. and Zeeshan Gul, M.: *Eur. Phys. J. Plus* **133**(2018)345; Sharif, M. and Naz, S.: *Mod. Phys. Lett. A* **35**(2020)1950340.
- [14] Ruderman, M.: *Annu. Rev. Astron. Astrophys.* **10**(1972)427.
- [15] Sokolov, A.I.: *J. Exp. Theor. Phys.* **49**(1980)1137.
- [16] Kippenhahn, R., Weigert, A. and Weiss, A.: *Stellar Structure and Evolution* (Springer, 1990).
- [17] Herrera, L. and Santos, N.O.: *Phys. Rep.* **286**(1997)53.
- [18] Harko, T. and Mak, M.K.: *Ann. Phys.* **11**(2002)3.
- [19] Paul, B.C. and Deb, R.: *Astrophys. Space Sci.* **354**(2014)421.
- [20] Ovalle, J.: *Mod. Phys. Lett. A* **23**(2008)3247.
- [21] Ovalle, J. et al.: *Eur. Phys. J. C* **78**(2018)960.
- [22] Gabbanelli, L., Rincón, Á. and Rubio, C.: *Eur. Phys. J. C* **78**(2018)370.
- [23] Sharif, M. and Sadiq, S.: *Eur. Phys. J. C* **78**(2018)410.
- [24] Estrada, M. and Tello-Ortiz, F.: *Eur. Phys. J. Plus* **133**(2018)453.
- [25] Singh, K. et al.: *Eur. Phys. J. C* **79**(2019)851.
- [26] Hensh, S. and Stuchlík, Z.: *Eur. Phys. J. C* **79**(2019)834.
- [27] Zubair, M. and Azmat, H.: *Ann. Phys.* **420**(2020)168248.
- [28] Maurya, S.K. et al.: *Phys. Dark Universe* **30**(2020)100640; Maurya, S.K. and Tello-Ortiz, F.: *Phys. Dark Universe* **27**(2020)100442; *ibid.* **29**(2020)100577; Maurya, S.K. et al.: *Eur. Phys. J. C* **81**(2021)848; Maurya, S.K., Tello-Ortiz, F. and Govender, M.: *Fortsch. Phys.* **69**(2021)2100099; Maurya, S.K., Tello-Ortiz, F. and Ray, S.: *Phys. Dark Universe* **31**(2021)100753.

- [29] Sharif, M. and Saba, S.: Chin. J. Phys. **59**(2019)481; ibid. **63**(2020)348; Int. J. Mod. Phys. D **29**(2020)2050041.
- [30] Sharif, M. and Waseem, A.: Chin. J. Phys. **60**(2019)426; Ann. Phys. **405**(2019)14; Sharif, M. and Majid, A.: Chin. J. Phys. **68**(2020)406; Phys. Dark Universe **30**(2020)100610; Sharif, M. and Naseer, T.: Chin. J. Phys. **73**(2021)179; Naseer, T and Sharif, M.: Universe **8**(2022)62.
- [31] Sharif, M. and Hassan, K.: *Anisotropic Decoupled Spheres in  $f(G, T)$  Gravity* Int. J. Geom. Methods Mod. Phys. (2022, to appear).
- [32] Shamir, M.F. and Ahmad, M.: Eur. Phys. J. C **77**(2017)674; Sharif, M. and Naeem, A.: Int. J. Mod. Phys. A **35**(2020)2050121.
- [33] Ilyas, M.: Eur. Phys. J. C **78**(2018)757; Maurya, S.K., Singh, K.N. and Nag, R.: Chin. J. Phys. **74**(2021)313; Sharif, M., Naeem, A. and Ramzan, A.: Astrophys. Space Sci. **367**(2022)21.
- [34] Krori, K.D. and Barua, J.: J. Phys. A Math. Gen. **8**(1975)508.
- [35] Güver, T. et al.: Astrophys. J. **719**(2010)1807.
- [36] Buchdahl, H.A.: Phys. Rev. **116**(1959)1027.
- [37] Andréasson, H.: J. Differ. Equ. **245**(2008)2243.
- [38] Ivanov, B.V: Phys. Rev. D **65**(2002)104011.
- [39] Mustafa, G. et al.: Chin. J. Phys. **67**(2020)576.
- [40] Herrera, L.: Phys. Lett. A **165**(1992)206.